ELSEVIER

Contents lists available at ScienceDirect

International Journal of Biological Macromolecules

journal homepage: www.elsevier.com/locate/ijbiomac





Water immersion behavior of CNF/GNP reinforced green epoxy hybrid nanocomposites

J. Yusuf ^a, S.M. Sapuan ^{a,*}, Umer Rashid ^{b,c,d}, R.A. Ilyas ^{e,f}, M.R. Hassan ^a

- ^a Advanced Engineering Materials and Composites Research Centre (AEMC), Department of Mechanical and Manufacturing Engineering, Universiti Putra Malaysia, 43400 UPM Serdang, Selangor, Malaysia
- ^b Institute of Nanoscience and Nanotechnology (ION2), Universiti Putra Malaysia, Serdang 43400, Selangor, Malaysia
- ^c Center of Excellence in Catalysis for Bioenergy and Renewable Chemicals (CBRC), Faculty of Science, Chulalongkorn University, Bangkok 10330, Thailand
- d Department of Chemical Technology, Faculty of Science, Chulalongkorn University, Pathumwan, Bangkok 10330, Thailand
- ^e Faculty of Chemical and Energy Engineering, Universiti Teknologi Malaysia, 81310 UTM Johor Bahru, Johor, Malaysia
- f Centre for Advanced Composite Materials, Universiti Teknologi Malaysia, 81310 UTM Johor Bahru, Johor, Malaysia

ARTICLEINFO

Keywords: Oil palm cellulose nanofibril Bio-based epoxy Graphene nanoplatelet Water absorption Raman spectroscopy

ABSTRACT

Environmental challenges have prompted the development of sustainable materials such as nanocomposites. However, these composites exhibit inadequate water resistance, leading to suboptimal performance. This study investigates the impact of water absorption on the properties of green epoxy nanocomposites reinforced with low loading of cellulose nanofibrils (CNF) and graphene nanoplatelets (GNP) at (0.1, 0.25, and 0.5) wt%. After 15 days of water immersion, contact angle tests showed that CNF increased hydrophilicity 80.26°, while GNP improved water resistance 90.04°. The presence of nanoparticles was confirmed by XRD and Raman spectra. Micrographs from FESEM confirmed the role of CNF in making nanocomposite hydrophilic due to water molecule penetration through capillary flow due to hydrolytic breakdown. Mechanical tests indicated a $46.6\ \%$ increase in hardness for water-absorbed hybrid nanocomposites, with GNP enhancing impact resistance, tensile strength ranging from 400 to 600 MPa and flexural strength between 600 and 800 MPa. Thermally, the composites offer conductivity values of 10-30 W/m·K, supporting efficient heat dissipation, and maintain structural integrity at temperatures up to 300 °C due to the synergistic effects of CNF and GNP. The GNP enhances interfacial bonding with the epoxy matrix through π - π stacking and van der Waals forces. Its high aspect ratio and 2D structure improve stress transfer, load distribution, and crack resistance. Additionally, GNP forms continuous thermal pathways, boosting thermal conductivity and heat dissipation. This study emphasizes that filler dispersion and component interaction play vital roles in defining density performance and water absorption and highlights the role of filler type and dispersion in controlling moisture behavior, offering the potential for moisture-resistant composites in electronics applications.

1. Introduction

Scientists are compelled to focus on research into different solutions using renewable and sustainable materials, obtained via efficient production strategies due to the growing depletion of fossil-based resources, excessive dumping [1] and growing ecological concerns [2–4]. The development of innovative materials such as bio-based composites [5] with appropriate techniques and the promotion of the diversification of energy are essential [6], for achieving the Sustainable Development

Goals of the United Nations by 2030. These materials should offer unique structural properties and outstanding attributes for their employment in numerous industrial domains [7]. Considering this, materials created by cellulosic matter with favorable intrinsic physical and chemical properties, good compatibility, biodegradability, and changeable performance can be utilized in various advanced fields [8,9]. In the medical, engineering, electronics [10], and environmental domains, bio-based materials have drawn a lot of interest and ongoing attention. This is especially the case when targeted structural techniques

^{*} Corresponding author at: Advanced Engineering Materials and Composites Research Centre (AEMC), Department of Mechanical and Manufacturing Engineering, Universiti Putra Malaysia, 43400 UPM Serdang, Selangor, Malaysia

E-mail addresses: sapuan@upm.edu.my (S.M. Sapuan), umer.rashid@upm.edu.my (U. Rashid), ahmadilyas@utm.my (R.A. Ilyas), roshdi@kelantanutilities.com. my (M.R. Hassan).

and suitable design concepts are paired together. It's interesting to note that the advancement of nanoscience and nanotechnology in recent decades has led to remarkable breakthroughs in hybrid materials created at the nanoscale or molecular level [11,12].

The polymer composites are enhanced by the addition of certain nanofillers. Depending on the type of nanofiller added and how well it works in conjunction with the other elements of the polymer composites, such as the matrix material or the fibers reinforcement. The addition of such nanofillers to the polymer composites can provide a variety of outcomes. One can either enhance the current properties of the polymer composite or introduce new properties. In polymer composites including natural resources, nanofillers are very helpful [13]. Plant based materials can be utilized to decrease the pollution which can counter the plastics [4,14]. The cellulose chains are separated into crystalline (ordered) and amorphous (disordered) portions; chemical treatments are typically used to eliminate the former. Nanocellulose is extracted from cellulose which is the most abundant natural resource in nature and has a one-dimensional morphological structure with an exceptional number of hydroxyl groups [15,16]. To extract nanofibers (CNF), nanocrystals (CNC), microfibrils (MFC), or microcrystalline cellulose (MCC), cellulose can be treated chemically or mechanically and have a vast applications in different fields [11,17]. Graphene as an allotrope of carbon is widely used in advanced nanocomposites. Graphene was discovered in 2004 by Andre Geim and Konstantin Novoselov [18,19]. Graphene nanoplatelets (GNPs) are a type of graphene material that is composed of stacks of graphene layers. They are usually between 5 and 50 nm in thickness and have a platelet-like shape and are used as nanofillers. GNPs exhibit superior electrical, mechanical, and thermal properties, the thermal conductivity of single-layer graphene can be up to 5000 W·m⁻¹·K⁻¹ [20]. By adding GNPs to polymers, it is practical to notably improve strength, stiffness, and resistance to fracture of resulting composite material [21-23]. GNPs are a promising family of graphene materials with numerous possible future high-end uses like energy storage devices and sensors [24-27]. Due to the formation of an efficient network of strains [28] which was confirmed by other researchers [29]. When nanocellulose and graphene derivatives (GNMs), either unmodified or surface-modified through various physical or chemical processes, are combined, the shortcomings of both are balanced out and the benefits of both are transferred, leading to several intriguing properties and uses [30,31]. Three main techniques are used to disperse nanomaterials: melt processing, in situ polymerization, and solution mixing. The scientific community has extensively acknowledged and found excellent results with solution blending and in situ polymerization. Melt processing is typically used in the plastics sector [32], although the grade of dispersion obtained using this technique is frequently inferior [33]. The vital properties of epoxy are widely employed in many applications [34].

Epoxy is extensively used for its mechanical properties and chemical resistance. Yet, it faces an environmental concern due to the toxic behavior of BPA resulting in the endangering of humans and animals [35]. This is fundamental in the context of escalating concerns regarding environmental pollution and the discharge of hazardous substances into aquatic ecosystems ascribed to synthetic polymers [36]. Thus, efforts are made to develop biopolymers from renewable resources like vegetable oils which are aimed at replacing BPA along with an added value. To be labeled as green or bio epoxy, the resin needs at least 25 % bio-content per USDA standards [37]. Epoxy composites, with epoxy resin serving as the matrix, are widely used as adhesives due to their strong bonds [38], versatility, and suitability for various applications, including aerospace, automotive, and electronics.

A newly developed bonding technique called adhesive joining joins several kinds of material together using an adhesive. The possibility of producing low-cost components, flexibility in joining dissimilar materials, even stress distribution, and comparatively less processing requirements are just a few of the advantages adhesive bonding offers over other joining techniques [39,40]. For epoxy resin, it has good

mechanical properties, convenient molding process and better bonding strength with the other medium, which can be used in the resin matrix, interface adhesive and coating for the repairing and strengthening of engineering structures [41]. However, polymer adhesive frequently has low resistance to moisture and humidity, which restricts its use in a larger variety of applications. Particularly, in humid environments, some polymeric adhesives tend to absorb moisture, which reduces interfacial adhesion and bonding effectiveness [38,42]. Adsorbed moisture or humidity may lead to plasticization or swelling, which in turn promotes the formation of interfacial cracks and reduces joining strength [43]. However, polymeric materials are susceptible to plasticization, a breakdown process triggered by moisture, as well as moisture absorption. This effect mostly results in the loss of matrix-dominated characteristics because the matrix is the only component in these composites that absorbs water [44].

Due to several significant benefits, the use of nanocomposite adhesives has been suggested as a solution to the issue. According to recent studies, nanocomposite adhesives have shown promising results for enhancing adhesive joining's tolerance to humidity [45]. Negar et al. [46] used SiO₂-based nanoscale ionic materials (SiO₂-NIMs) into a novel epoxy (EP) nanocomposite adhesive to improve its strength, transparency, and heat stability. It was found that through electrostatic interactions and hydrogen bonding, NIMs enhanced interfacial bonding, stiffness, and toughness. It also increased shear strength and crack resistance. By impeding polymer plasticization and swelling, nanocomposite adhesives have demonstrated the ability to decrease water uptake and moisture absorption rate while maintaining bonding strength. This is attained from following technique: i) Nano additives form a twisting channel by obstructing water diffusion, which reduces the rate of diffusion; or ii) the formation of a chemical interface among nanoparticles and substrates reduces water diffusion, which preserves joining performance [47].

Assessment of the potential of nanocomposites adhesive in improving the bonding performance and humidity resistance of adhesive joining has been conducted to a considerable extent. For instance, Ahmad et al. [48] demonstrated that adding graphene nanoplatelets (GNP) and multiwalled carbon nanotubes (MWCNT) improves the mechanical properties of glass-reinforced epoxy composites while decreasing their water absorption. A 1.5 % GNP-MWCNT hybrid improved tensile and flexural strengths to 269.3 MPa and 294.4 MPa, respectively, and enhanced water-aging resistance and self-sensing capabilities. Similarly, Oun et al. [49] reported that 0.5 % graphene exhibited the least reduction in inter-laminar and flexural shear strengths following prolonged exposure. In hybrid natural fibers composites, graphene nanoparticles have also been shown to improve mechanical properties and reduce moisture absorption.

Shettar et al. [50] reported that adding nano clay to epoxy composites improved their mechanical properties and reduced their absorption of water, leading to a 90 % recovery in the composites tensile and flexural strengths after desorption. Epoxy-nano clay nanocomposites (ENNCs) demonstrated a reduced drop in strengths during water sorption-desorption-resorption conditions in comparison to pure epoxy. According to research conducted by Venkatesan et al. [51] hybrid composites consisting of epoxy resin and coir fibers mat reinforced with nano-silica particles exhibit better mechanical properties and less water absorption. Notably, in terms of reducing water absorption, the composite containing 20 % nano-silica coir mat shown the better overall outcomes. In a study by Singh et al. [52] they reported that water resistance of an epoxy composite was significantly increased when annealed nanodiamond (ND) particles were added. As the ND concentration (0.1, 0.3, and 0.5 wt%) increased, the composite's water absorption and contact angle reduced, suggesting improved water resistance due to a decrease in epoxy chain mobility and hydrogen bonding between ND and epoxy.

It was reported by Prasad et al. [53] that the mechanical characteristics and water resistance was significantly improved by 22 % and

24 %. The results also showed 16 % increase in tensile, flexural, and interlaminar shear strengths. For samples with a 0.6 wt% TiO2 coating, the water diffusion coefficient decreased by 42 %, indicating improved water absorption resistance because of nanoparticle grafting and silane treatment on the fibers surface. The study carried by Utaman et al. [54] demonstrated that adding MWCNTs modified with surfactants to an epoxy matrix greatly enhanced its mechanical characteristics and decreased its absorption of water by improving the dispersion of CNTs and interfacial bonding. Nevertheless, greater CNT concentrations (over 1.5 %) caused agglomeration, which enhanced the absorption of water by creating voids and microcracks. Chandel et al. [55] examined the water absorption and rupture energy of epoxy composites in various aqueous settings. After preliminary findings, it was discovered that moisture absorption rates varied with the medium, exhibiting non-Fickian behavior. In contrast to specimens in air, which displayed no weight change because of low diffusivity, specimens in normal water, half-saturated, and fully saturated salt solutions showed enhanced moisture absorption. The use of adhesives in nanocomposite composites for humidity resistance and the ensuing bonding strength of adhesive joining has shown several noticeable trends. These changes may be affected by various aspects, including the type of nano reinforcement used, the optimal content of nano additives, and the dispersion behavior of the nanostructure in polymer matrix.

Several research has been done on absorption of CNF and GNP in synthetic based epoxy composites. However, no work in the past has been done on CNF, GNP and their hybrid using a bio-based epoxy with low loadings. The current study examines effects of water absorption on physical, mechanical and morphological properties of oil palm cellulose nanofibril/graphene nanoplatelet reinforced green epoxy hybrid nanocomposites. This research will play a vital role in the development of water retardant hybrid composites with an improved mechanical property due to the loading of GNP. The nano composites can be used in under water electronics equipment.

2. Materials and methods

2.1. Materials

The green epoxy resin, SR Green Poxy 28 (Part A), was supplied by Mecha Solve Engineering, Selangor, Malaysia together with the hardener, SD 3304 (Part B). At 30 °C, the viscosity of green epoxy was 4500 mPa s, its density was 1.17 ± 0.01 and its gel time was 3.45 h. GNP was acquired from Malaysia's GO Advanced Solutions Sdn. Bhd., Malaysia. Black or grey powder, with a thickness of 0–2 nm, carbon content of >99 %, an apparent density of 0.06-0.09 g/mL, a water content of <2 %, and residual impurities of <1 %, was how GNP appeared. Oil palm CNF that had been spray-dried was acquired from Zoepnano Sdn. Bhd., Putra Science Park, Malaysia. CNF had an opaque white physical appearance. The nanocellulose had a 99 % concentration, a neutral pH, a diameter of <50 nm, a DLS of 40 nm to 25 nm, an onset temperature of about 300 °C, and a total deposition temperature of around 600 °C. Acetone was utilized as the dispersion solvent.

2.2. Fabrication of bio nanocomposites

By adopting solution blending in four fundamental stages, the GNP/CNF reinforced green epoxy hybrid bio nanocomposites were fabricated: sonicating the nanoparticles to dissolve them in the solvent; addition of polymer solution; mixing some more; and finally, evaporating solvent to remove it. A digital balance (AND GF-1000, Japan) with a readability of 0.01 mg was used to weigh combined GNP/CNF with varying weight percentages, such as (0.1, 0.25, and 0.5) wt%. It was distributed in 100 mL (0.1 g) of acetone in a 1000 mL glass beaker. The suspension was then sonicated (Digital Pro+, Malaysia) for two hours at 25 °C, using an ice bath to hold the water's lower temperature. After the sonication, suspension was left undisturbed for a while to observe sedimentation

behavior. Uniformly dispersed suspension was made sure, which showed zero settling of GNP/CNF particles.

The method for making GNP/CNF reinforced green epoxy hybrid nanocomposites are depicted in Fig. 1. After adding green epoxy, the acetone and GNP/CNF mixture was once more sonicated for two hours. After that, the mixture was kept at 75 °C for 2.5 h using a lab hot plate (Faithful Instrument, China) for evaporate the acetone. Green epoxy and GNP/CNF were continuously mixed for 30 min at 500 rpm using a mechanical stirrer (IKA RW 20, Malaysia). Part B of the green epoxy, the curing hardener, was combined with water in an 8:2 ratio and stirred by hand for five minutes. A 200x200x3.0 mm steel mold was previously prepared by applying mold release wax (Meigura's mirror glass) three times, separated by 30 min. Poured mixture was allowed to precure at room temperature for sixteen hours in a steel mold. For a seven-hour post-curing period, the mold was placed in an oven set at 90 °C. After the sheet was taken out of the mold, samples were made for testing using a vertical bandsaw (Makita LB1200F, Japan) with a 165 mm cutting depth.

2.3. Testing

2.3.1. Water absorption tests

The moisture specimens were precisely weighed with an analytical digital scale to within 0.001 grammes. The samples were submerged in deionized water and kept at room temperature (25 $^{\circ}$ C) for an interval ranging from 5 to 15 days. The samples were submerged in a confined container during a stationary procedure known as immersion. Before final weight was recorded, the specimens were hand dried using tissue paper. Eq. 1 was used to calculate the nanocomposite water uptake.

Water uptake,
$$M_t$$
 (%) = $\frac{W_f - W_i}{W_i} \times 100$ (1)

where W_f and W_i are the sample final weight following the appropriate immersion period and sample initial weight, and M_t is the amount of water absorbed at time at a certain immersion period.

2.3.2. Water density tests

The Mettler Toledo XS205 water density testing machine utilizes a $10\ \mathrm{cm}^3$ calibrated glass sinker, suspended by a platinum wire, for gravimetric density determination of liquid samples. A calibrated thermometer was included for accurate temperature monitoring during the density tests.

2.3.3. Contact angles

A Theta Lite (Biolin Scientific, Sweden) was used to measure the composite surface's contact angle. By affixing the samples ($25 \times 25 \times 3$ mm) to sample holder and applying sessile drop technique to sample surface, contact angle of the samples was determined. After 10 s of contact angle measurement, a picture clicked right away.

2.3.4. Chemical analysis

To classify functional groups, present in CNF/GNP reinforced green epoxy hybrid nanocomposites, Fourier transform infrared spectroscopy (FTIR) was performed using a Thermo Fisher Nicolet iS10 spectrophotometer, Universiti Putra Malaysia. The analysis is completed within a frequency range of 400 to 4000 ${\rm cm}^{-1}$, operating at a resolution of 4 ${\rm cm}^{-1}$. The fracture surfaces were sputter coated with platinum for 50 s using Sputter Coater (Model: K575X, UK) to allow an excellent surface morphology observation. FTIR measurements included acquiring spectra through 16 scans, with a scan speed of 0.47 cm/s. These experiments were intended to characterize the hybrid nanocomposites and determine the specific functional groups associated with the CNF/GNP component.

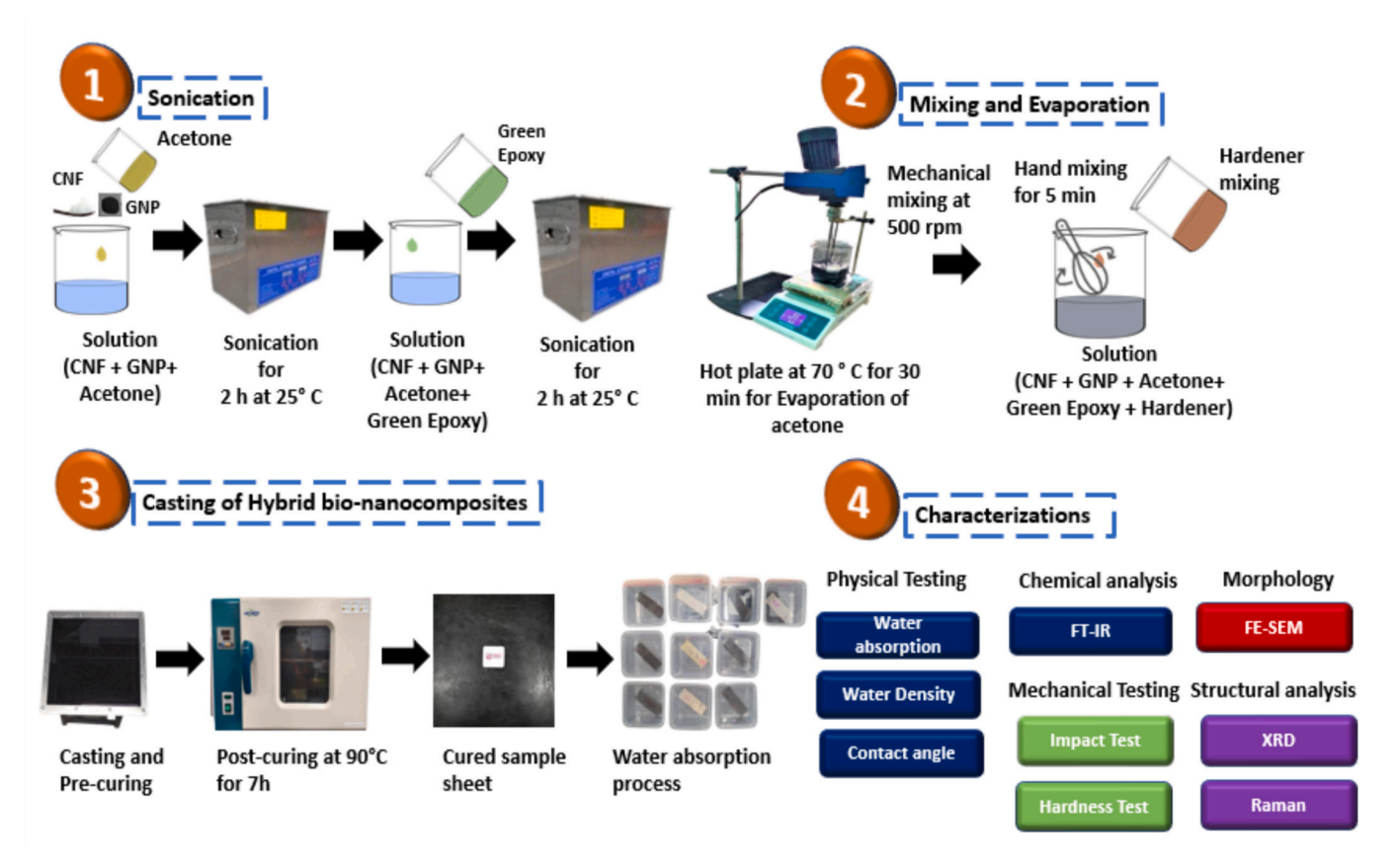


Fig. 1. Methodology for preparation of CNF/green epoxy nanocomposites and their testing.

2.3.5. Morphological analysis

A 5.0 kV-powered field-emission scanning electron microscope (Nova Nanosem 230 FESEM, Netherlands) was used to analyze the microstructure of the nanocomposites. To improve surface morphology observation, the fracture surfaces were sputter coated with platinum for 50 s using a high vacuum sputter coater, which gave samples electrical conductivity.

2.3.6. X-ray diffraction (XRD)

MiniFlex 600 (Japan) and Rigaku SmartLab (2) were used for XRD testing at 25 °C, 40 kV, and 30 mA. From $2\theta=5^\circ$ to 60° , the samples (20 \times 20 \times 3 mm) were scanned.

2.3.7. Raman spectra analysis

The Raman shift was examined using the WITec Alpha 300R Raman Spectrometer, which was set up with a grating of 600 g/mm (BLZ $=500\,$ nm) and an excitation wavelength of 532.066 nm. Its spectral centre is 1997.607 cm $^{-1}$, and its centre wavelength is 595.342 nm. It has a 0.05 MHz horizontal shift speed and an 8.25 μs vertical shift speed.

2.3.8. Rockwell hardness tests

The nanocomposites' mechanical properties included impact strength and Rockwell hardness. Each test involved five samples, and when required, the average value and standard deviation was determined. The Rockwell F hardness test was employed to assess the hardness of polymer nanocomposites using a digital hardness tester. The dimensions of the test specimens were 25 mm \times 25 mm in accordance with ASTM 1)785 [35]. A steel ball with a diameter of 1/16-in. was utilized at a load of 490 N for a duration of 5 s.

2.3.9. Impact tests

The amount of energy absorbed prior to rupture of the polymer

nanocomposites was measured using the Charpy test. The impact strength was determined using a machine (Gunt Hamberg, Germany). ASTM D256 standard [56] was used to gauge impact strength of polymer nanocomposites. The size of samples was (65 \times 15 \times 3) mm.

3. Results and discussion

3.1. Water absorption tests

3.1.1. Water absorption of CNF reinforced green epoxy nanocomposites

As CNF has a high surface area to volume ratio and many available hydroxy groups, it absorbed a large amount of water. Moreover, as CNF networks enlarged, even more surface is exposed, increasing the quantity of hydroxy groups that can be absorbed by water. The accessibility of hydroxy groups has been linked to the rate of sorption and desorption of water in CNF since they were the main sites of contact for water on the surface [57]. The degree of aggregation, geometric limitations, porosity and the thermal history of the nanocellulose were some of the elements that controlled accessibility. Due to the network's flexibility, remaining lignocellulosic components like hemicellulose, and increased hydroxy group accessibility, CNF has a generally higher water vapor uptake capacity.

The water uptake in 0.25 wt% CNF was high and reached to 9.483 g from 6.653 g as observed in Fig. 2. Poor fiber-matrix interfacial bonding resulted from an increase in fiber loading. A reduction in the mechanical properties of bio-composites due to water uptake was also reported [58]. Water resistance of CNF/epoxy composites with low epoxy loading had higher water absorption [59]. However, in long-term weight reduction from 9.456 g to 6.933 g in CNF epoxy composites was due to water absorption. It primarily caused by plasticization, swelling of the matrix, and interfacial damages leading to reduced mechanical properties which can be seen in day 10 to day 15 in 0.5 wt% of CNF.

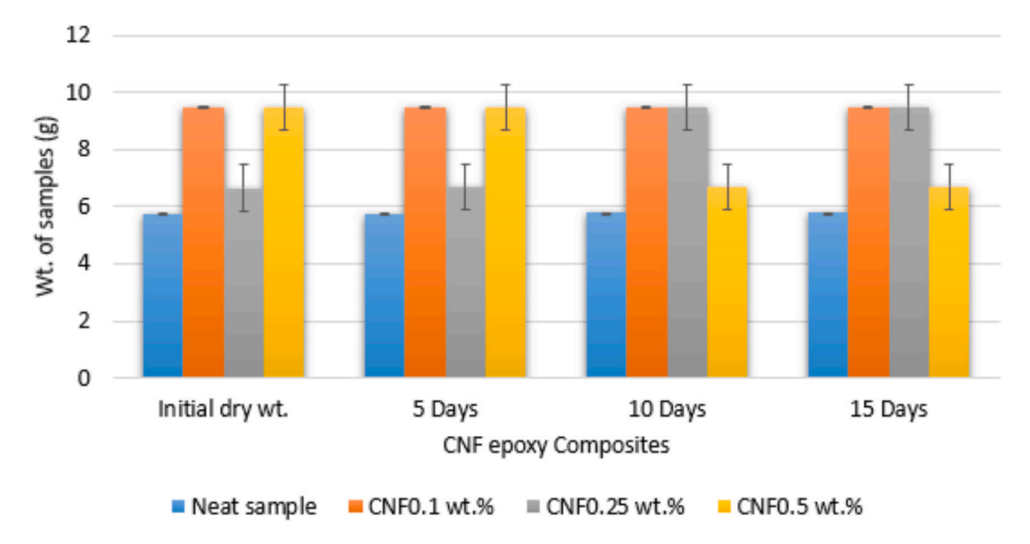


Fig. 2. Water absorption test data of different CNF loadings.

Classic diffusion controlled by local variations in chemical potential—that is, when the pore size is big, and the porosity is high—is referred to as Fickian diffusion. In these situations, the interactions between the diffusing molecule and the solid substance are negligible. Conversely, Knudsen diffusion happened when the solid material's pore size is equal to or less than the diffusing molecule's mean free path, resulting in substantial interactions between the solid and the vapor which might be the cause of rise in weight content in wt% of CNF in day 10 to 15. Subjected to the porosity, pore size, and surface energy of the nanocelluloses, water vapor mass transport across them may involve any one of these methods [60] [61]. While CNF is primarily hydrophilic and can increase water absorption, its role in thermal conductivity is also significant.

3.1.2. Water absorption of GNP reinforced green epoxy nanocomposites

Neat sample had constant amount of water absorption throughout the duration as compared to GNP which was hydrophobic in nature and repelled the water absorption [62] (refer to Fig. 3.).

In comparison to neat epoxy, GNP nano composites with $0.1~\rm wt\%$ had the least amount of water absorption. The value of all water absorption increased together with the GNP exhibit in the composites. On

day 15, it was found that GNP composites with 0.25 wt% and 0.5 wt% GNP had the maximum water absorption values. Due to non-homogeneous dispersion and aggregation of nanoparticles the water absorption increased. This could be explained by the composites free volume and voids. In composites, a high weight percentage of GNP loading frequently results in incorrect dispersion. It resulted in higher void content in the high GNP loaded samples, which is what essentially raised the water absorption in the GNP-filled composites [63]. The increase in water uptake can potentially explained by the nanostructure content not being high enough to inhibit water uptake into the system, which would change the curing behavior and sections of the molecular packing polymer chain while wet. Increased GNP loading into the polymer matrix might have aided in the barrier mechanism, reducing the water permeability of the nanocomposite glue and increasing its effectiveness in inhibiting water absorption [64].

However, the increased rate of water absorption at shorter immersion times—5 days—may be the consequence of water molecules filling already-existing gaps in the polymer matrix, which causes the tiny micro-voids to rearrange and absorb water molecules into the samples much more quickly [65,66]. As the immersion times were prolonged, the gaps that the water molecules had occupied may have reduced the

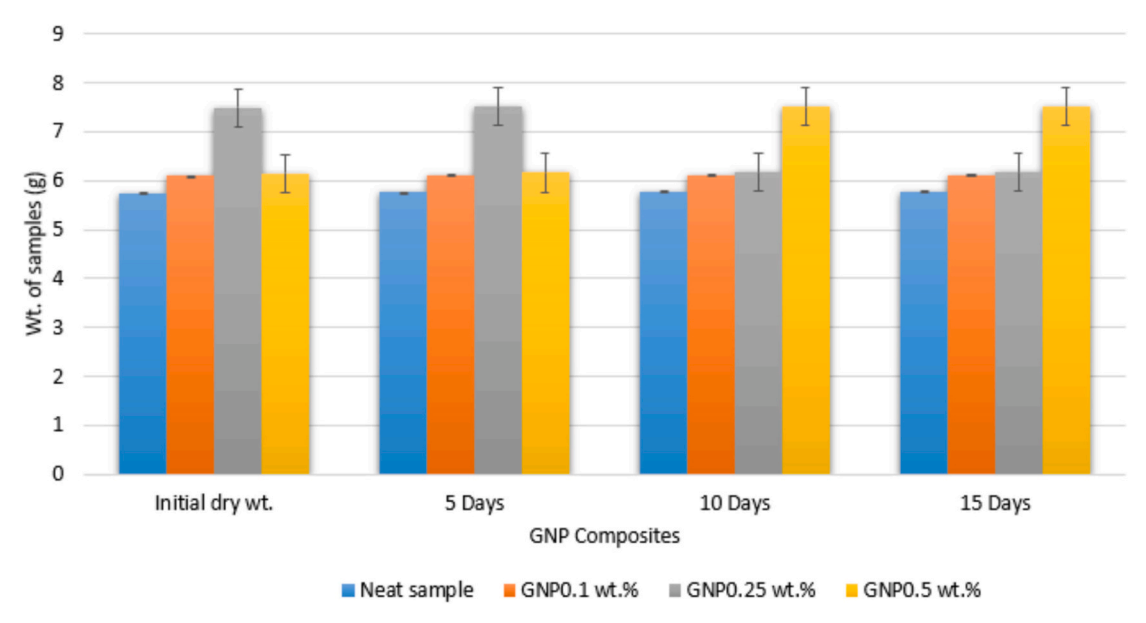


Fig. 3. Water absorption test data of different GNP loadings.

ability of the water molecules to diffuse, as has been observed in the sample with GNP 0.1 wt% on day 15. A decreased water absorption rate may have resulted from the appropriate quantity of nano reinforcement, as fewer water molecules were able to pass through the epoxy matrix [43]. The interaction between GNP and the epoxy matrix is crucial. Improved interfacial adhesion between GNP and the polymer matrix enhances the transfer of thermal energy. This is attributed to the effective dispersion of GNP within the epoxy, which minimizes thermal resistance at the interface, thereby improving overall thermal conductivity.

3.1.3. Water absorption of CNF/GNP hybrid reinforced green epoxy nanocomposites

CNF/GNP hybrid composites reduced water absorption in epoxy materials due to their unique properties such as barrier effect, low permeability, enhancing their potential in various applications such as sensing and wastewater treatment [67]. Water absorption was constant throughout the duration of the test which can been seen from the graph in Fig. 4. The neat sample was least affected from the water. The inherent properties of the epoxy resin, such as its crosslink density and chemical structure reduces the water absorption [68]. However, the remaining samples H (hybrid) 0.1 wt%, 0.25 wt% and 0.5 wt% showed an increment in the weight due to water absorption. This is because CNF in the hybrid composite is inherently hydrophilic, meaning it has a natural affinity for water. When incorporated into the epoxy matrix, it attracted and retained the moisture, leading to increased water absorption [69]. The specimens with GNP reinforcement had better interphase adhesion between polymer phases due to enhanced chemical interactions and surface/contact area between GNP and polymer matrix, as evidenced by the greater region in these specimens also constituted the increased water absorption in hybrid composites [43].

The dispersion of CNF and GNP within the epoxy matrix was critical. Poor dispersion could lead to agglomeration, which creates regions that are more susceptible to water absorption which might be the result of constant water absorption through the duration [68].

Several key differences and interactions were observed in the study of water absorption in cellulose nanofibril (CNF), graphene nanoplatelet (GNP), and hybrid composites. The inherent properties and dispersion of the fillers within the epoxy matrix influence the water absorption behavior of the nanocomposites. Neat epoxy exhibited the least water uptake due to its high crosslink density and hydrophobic chemical

structure. In contrast, CNF's hydrophilic nature, credited to its abundant hydroxyl groups, improved water absorption in hybrid samples. GNP improved water resistance, evidenced by a higher contact angle (90.04°), but also improved interphase adhesion, which in some cases contributed to localized water uptake. Poor dispersion, especially at higher filler loadings, led to agglomeration, creating micro voids and pathways for water ingress. This was reflected in the constant water absorption observed over the test period. Overall, CNF increased hydrophilicity, while GNP acted as a moisture barrier, and their combination resulted in a complex interplay affecting the composite's moisture behavior. Thus, the type of filler, its interaction with the matrix, and its dispersion quality are critical to optimizing water resistance in hybrid nanocomposites. The hydrophilic nature of CNF may also contribute to capillary action, which can facilitate the movement of heat through the composite. Although CNF increases moisture absorption, its interaction with GNP can create a complex network that aids in thermal management, especially in applications where heat dissipation is critical.

3.2. Water density

The density in neat sample before and after the absorption test did not change much due to epoxy's hydrophobic nature as shown in Fig. 5.

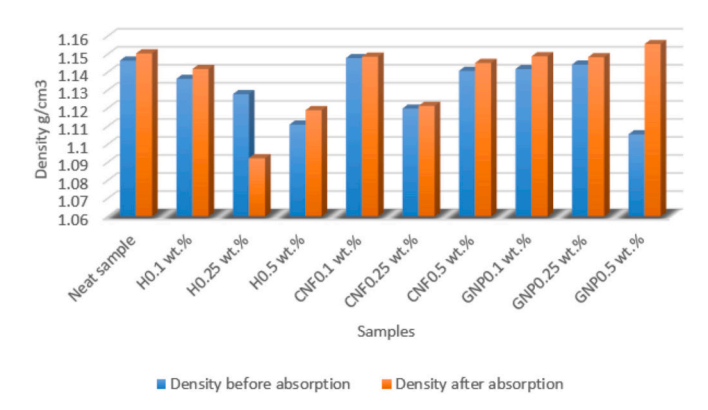


Fig. 5. Water density test data of different CNF, GNP and CNF/GNP hybrid composite loadings.

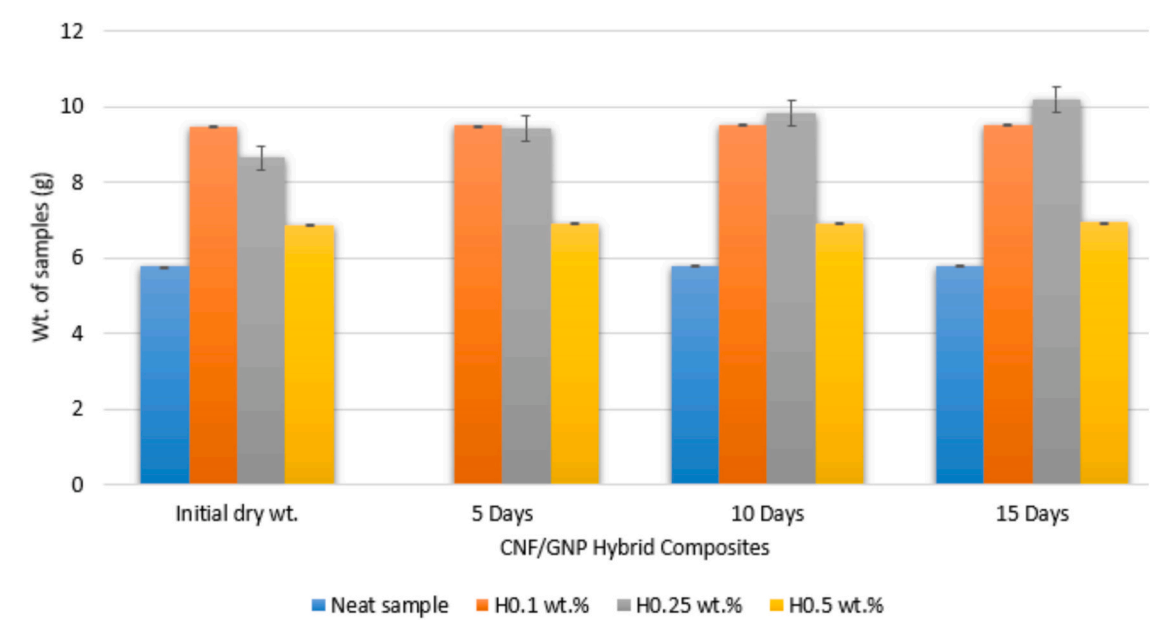


Fig. 4. Water absorption test data of different CNF/GNP hybrid composites loadings.

In general, epoxy resins repel water due to their hydrophobic nature. Due to this reason less water was absorbed, [70] which leads to very slight change in density. This property can keep the composite's density stable by limiting the amount of water absorption. The change was slight in hybrid composite 0.1 wt%. This was because CNF is naturally hydrophilic, it absorbs water easily. This caused the composites to inflate and increase in volume overall, which would change the density of the composites [71]. Another possible explanation is interplay between GNP and CNF in the epoxy matrix can produce channels or micro voids that make it easier for water to enter. This may result in increased density and increased absorption of water [72].

However, in hybrid 0.25 wt% water causes CNF to swell, which disturbed the composite's structure and lower its density. There was inadequate bonding between the CNF and the epoxy matrix, which resulted the swelling to become more noticeable which led to decrease in density of the hybrid composite. The change in CNF epoxy composite was not significant. Similar pattern was observed in 0.1 and 0.25 wt% GNP loading. However, major change was observed in 0.5 wt% of GNP. As GNP can open passageways for water molecules to enter the composite. Increased water absorption may result from this, particularly if the composite had voids or the GNP were not evenly distributed. Water infiltration was facilitated by the micro voids or channels that may be created by the interaction of GNPs with the epoxy matrix. This resulted in altered density and increased absorption of water, which further lead to an increase in density of the composites.

3.3. Water contact angles

The magnitude of the contact angle was used to describe the surface hydrophilicity and hydrophobicity of different composites, it analyze the stability and connectedness of liquid spreading over solid surfaces, and characterize the angle at which a liquid contacts a solid surface, directly reflecting the characteristics of the solid-liquid interface [73]. Cellulose and hemicellulose's amorphous structures allow water molecules to enter the fibers more easily, breaking intermolecular hydrogen bonds and exhibiting hydrophilic behavior [74]. Water has the highest affinity for both native and acetylated cellulose, resulting in low contact angles of 84.26° and 80.26° that indicate hydrophilic behavior. This facilitated the penetration of water into CNF networks, enhancing their interaction with aqueous environments [75]. A significantly increased water sorption capacity per mass of cellulose was the result of the isotropic character of most CNF networks and the notable rise in specific surface area (SSA). Increasing SSA also made surface hydroxy groups more accessible, which facilitates their easy interaction with water.

Additionally, the incorporation of charged groups onto the nanocellulose's surface during isolation will change how it interacts with water. The interaction between CNF and water was a phenomenological process that includes several overlapping phenomena, including hydration, condensation, wetting, and diffusion, (refer Fig. 6). These phenomena are all mediated by different interaction forces, such as van der Waals forces, hydrogen bonds, and electrostatic interactions. CNF remarkable hygroscopic properties were ultimately caused by these activities, which took place throughout various length scales [61].

The use of GNP as nanofillers in composites worked as a barrier, making composites absorb less water. Hence, plays a major role in reducing water absorption rate, which can be observed in Fig. 7 the loadings of GNP were directly proportional to the contact angle [76] at 0.1 wt% GNP loading the contact angle was 75.07°, at 0.25 wt% the contact angle was 90.07° and at 0.5 wt% the contact angle was 94.07° . The water vapor permeability (WVP) in nanocomposites diminished asymptotically with elevated GNP concentrations across all composites. Larger lateral GNP sizes were hypothesized to be more confined and partially aligned within the polymer matrix. The perpendicular orientation of GNP to the water vapor flow contributed to an increased tortuous pathway for water vapor molecules. Consequently, the drop in permeability for GNP was amplified relative to GNP-loaded systems, where higher GNP concentrations yield even lower barrier properties. Similar pattern was seen in hybrid nano composites in Fig. 8, where the effect of CNF was overshadowed by the GNP the contact angle was recorded as 90.07° and 94.04°. Interestingly, there was a relationship between the nanocomposite's permeability and viscosity. Permeability decreases when GNP concentration rises because matrix viscosity rises above a particular threshold. The abrupt increase in viscosity was described as the rheological percolation threshold, which shows the critical concentration at which the matrix viscosity abruptly increases due to the strong physical interaction between the nanoparticles, inhibiting polymer chain mobility [77]. High viscosity impairs matrix workability. The overall WVP and mechanical performance of the nanocomposites were influenced by exfoliation degree and rheological percolation threshold. Exfoliated platelets with minimal viscosity provided optimal performance. These conditions were satisfied at low GNP concentrations [78].

3.4. FTIR analysis

The chemical composition of GNP reinforced green epoxy nanocomposites were analyzed after submerged in water for 15 days, as shown in Fig. 9. It was carried to examine how the chemical

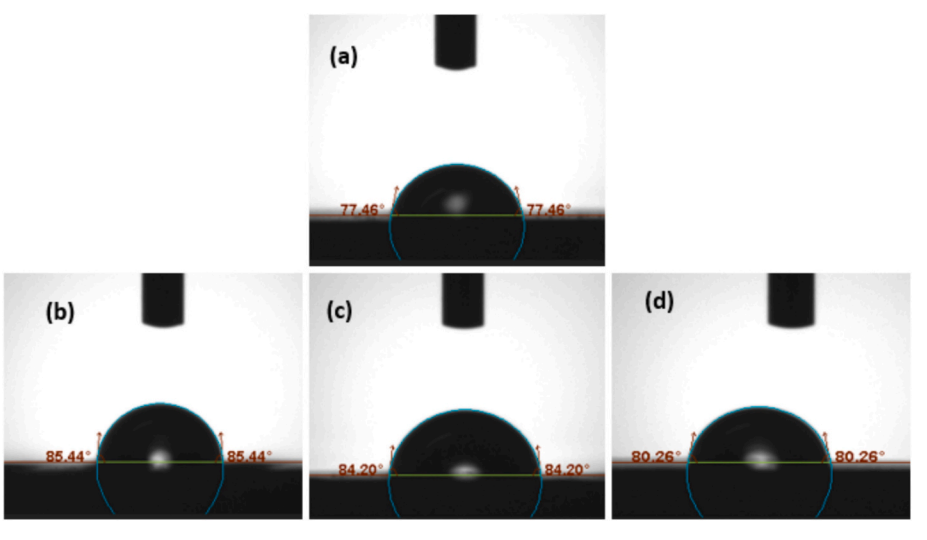


Fig. 6. Contact angle on water absorbed bio nanocomposites (a) neat sample (b) 0.1 wt% CNF loading (c) 0.25 wt% CNF loading, (d) 0.5 wt% CNF loading.

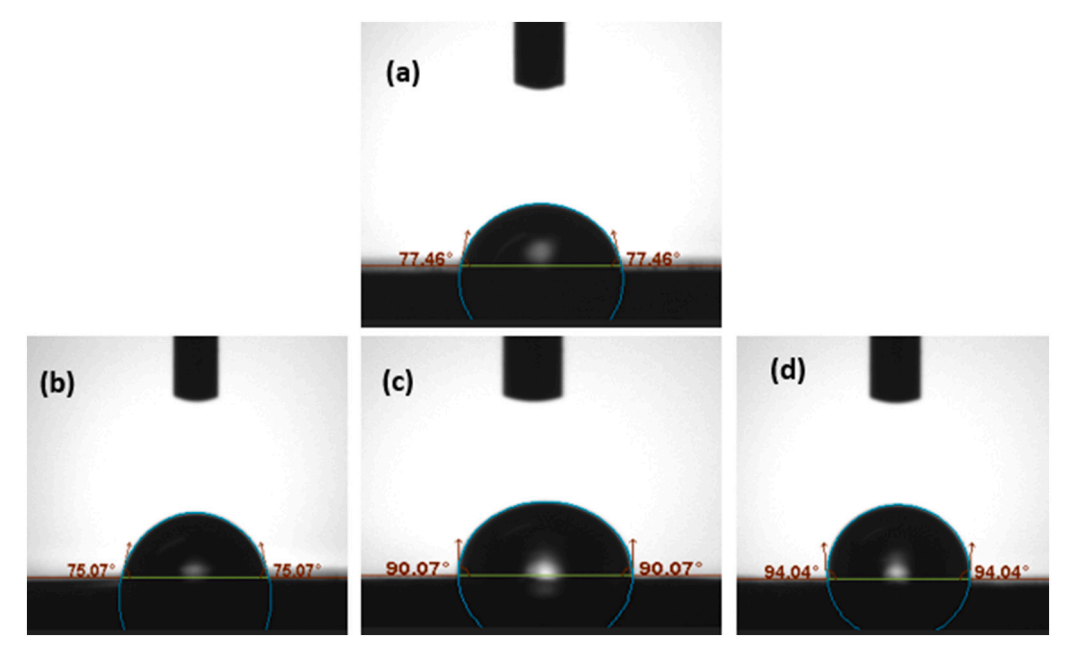


Fig. 7. Contact angles on water absorbed bio nanocomposites (a) neat sample (b) 0.1 wt% GNP loading (c) 0.25 wt% GNP loading, (d) 0.5 wt% GNP loading.

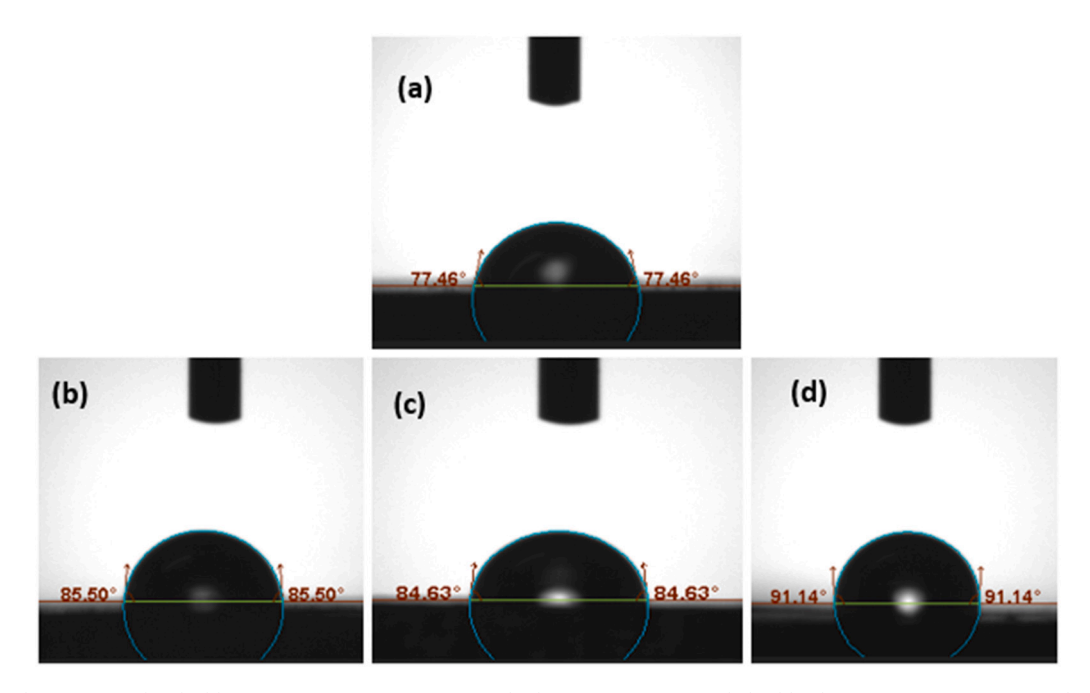


Fig. 8. Contact angles on water absorbed bio nanocomposites (a) neat sample (b) 0.1 wt% CNF/GNP hybrid loading (c) 0.25 wt% CNF/GNP loading, (d) 0.5 wt% CNF/GNP loading.

compositions and structures of the composites changed with 15-day immersion at different CNF and GNP loadings as compared to neat sample. The FTIR curve in Fig. (a) exhibited no peak variation after 15 days of immersion contrasted to neat sample. The O—H stretching vibration at 3000–3600 ${\rm cm}^{-1}$ indicates hydroxyl groups, suggested moisture presence due to absorbed water molecules or hydrogen bonding with matrix functional groups. Overall, no significant change was observed. This shows that the chemical compositions did not modify notably when the samples were submerged in water.

All CNF/green epoxy nanocomposites exhibited similar FTIR spectra across varying filler loadings. The absence of characteristic stretching vibrations at 845–820 ${\rm cm}^{-1}$ and 1350–1275 ${\rm cm}^{-1}$ indicated full curing of the epoxy moieties in all nanocomposites. FTIR spectra consistently

showed strong bands at 3000 cm⁻¹ and 950 cm⁻¹ associated with epoxide groups. The peak around 1500 cm⁻¹ was likely due to carboxylic group addition to primary alcoholic groups on CNF surfaces, observed in all nanocomposites [79]. This observation confirmed effective CNF incorporation into the epoxy matrix [80]. Olsson et al. reached the same conclusion as they identified two types of hydrogenbonded water associated with the O—H groups of cellulose and hemicelluloses [81].

An intense peak around 3607 cm⁻¹ was seen for all samples due to O—H stretching vibrations of the hydroxyl group in green epoxy resin; addition of CNF and GNP enhanced these hydroxyl group vibrations. The bands located between 32,100 cm⁻¹ and 3500 cm⁻¹ were attributed to the presence N—H stretching of primary and secondary amine of

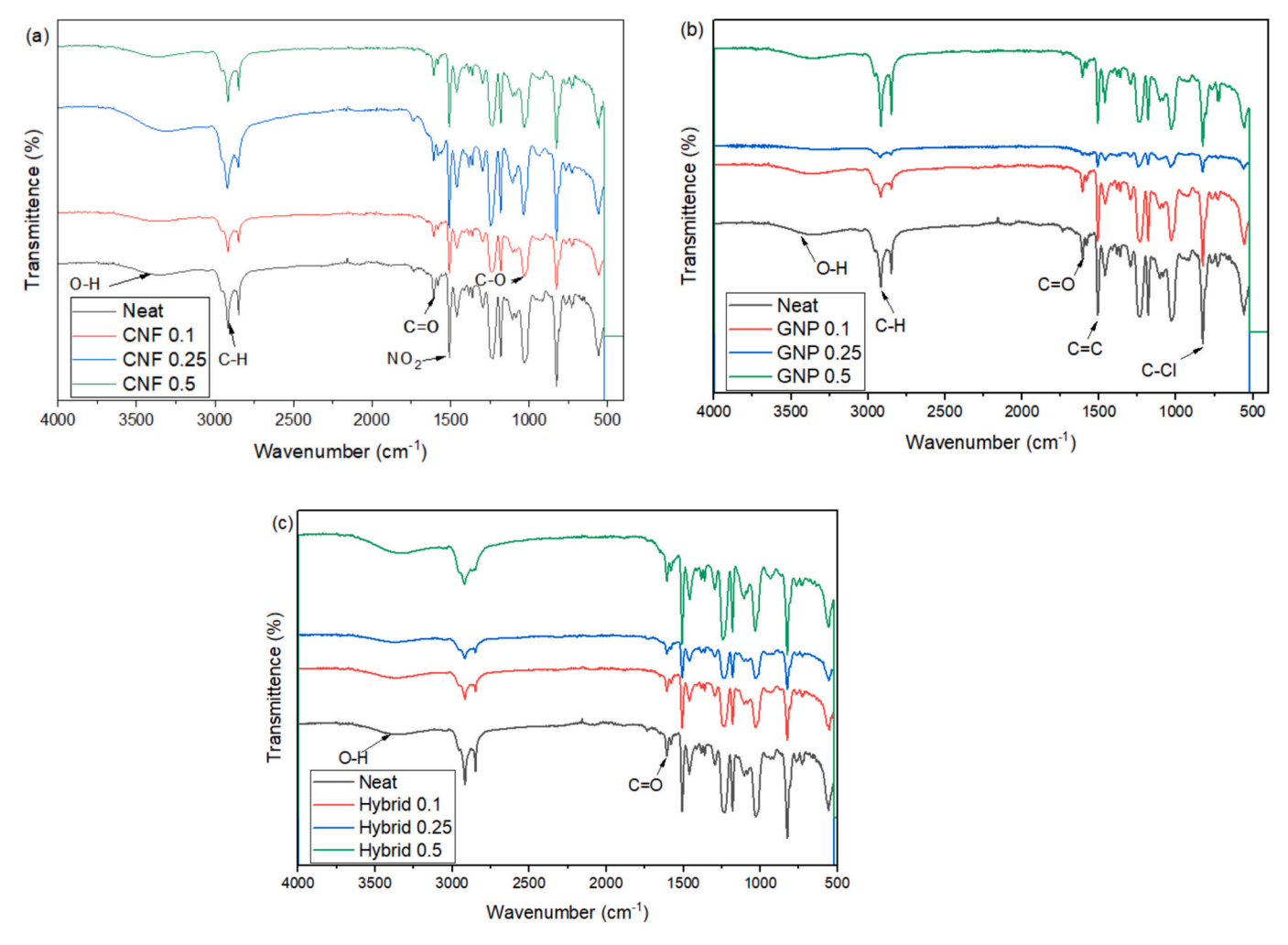


Fig. 9. FTIR spectra of water absorbed bio nanocomposites (a) 0.1,0.25 and 0.5 wt% CNF loadings (b) 0.1,0.25 and 0.5 wt% GNP loadings, (c) 0.1,0.25 and 0.5 wt% CNF/GNP hybrid loadings.

hardener. The intense peak at 1533 cm⁻¹ signified the N—H deformation of primary amine of hardener used for epoxy resin and silanetreated GNP and CNF, and intensity was reduced after loading of CNF and GNP, since few amino groups did not participate in ring opening polymerization reaction with epoxy group due to restacking tendency of GNP and agglomeration of CNF [82]. For binary nanofillers reinforced composites, the intensity was greater than that of the individual nanofiller-reinforced composite; this might be due to reduction of stacking tendency of GNPs. The emergence of a peak at 1327 cm⁻¹ represents distorted stretching vibrations of C—H group [83].

Water absorption in nanocomposites reinforced with cellulose nanofibrils (CNF) and graphene nanoplatelets (GNP), are greatly affected by the hydrophilic nature of the materials, as shown above through contact angle assessments. A low contact angle signifies an increased hydrophilicity of the material, thereby promoting the penetration and absorption of water due to the amorphous configuration of cellulose that facilitates the disruption of intermolecular hydrogen bonds. FTIR further clarifies these interactions by locating the functional groups engaged in water absorption, including hydroxyl groups, which are pivotal for the hydrophilic characteristics exhibited by the composites. The existence of these functional groups, coupled with the structural attributes of the nanocomposites, influences their water vapor permeability (WVP) along with their overall mechanical performance. It was seen that the incorporation of GNP improves water resistance, resulting in elevated contact angles and diminished water absorption.

3.5. Morphological analysis

As epoxy resins were prone to absorb moisture, swelling and plasticization may result in a decreased mechanical performance. The network architecture of the epoxy affected the absorption behavior, and Fig. 10(a) shows how changes in curing conditions impacted moisture uptake. The chemistry and microstructure of polymers were the main determinants of moisture sorption. Three mechanisms underlay moisture diffusion in polymer composites: transport through microcracks in matrix from production processes, moisture transfer through gaps and defects at fiber–matrix interface as a result of inadequate initial wetting and impregnation, and diffusion of water molecules in micro-gaps between polymer chains [84].

The investigation of water absorption in different loading of CNF epoxy nano composites revealed significant impacts on mechanical properties. Water absorption leads to debonding at the fiber-matrix interface, which is critical for maintaining composite strength. It was evident from the micrograph of FESEM (refer to Fig. 10(b)) that water absorption affected the fibers and disrupted bonding at the fiber-matrix interface, leading to reduced mechanical performance [85]. The findings were similar to Qing et al. [86] who also reached the same conclusion that found that CNF composites exhibit hygroscopic behavior, absorbing moisture that can lead to swelling and internal stresses within the matrix. It was evident as the composites were loaded with more fibers, they exhibited superior fiber-matrix interfacial bonding compared to those loaded with less fibers. Composites with a

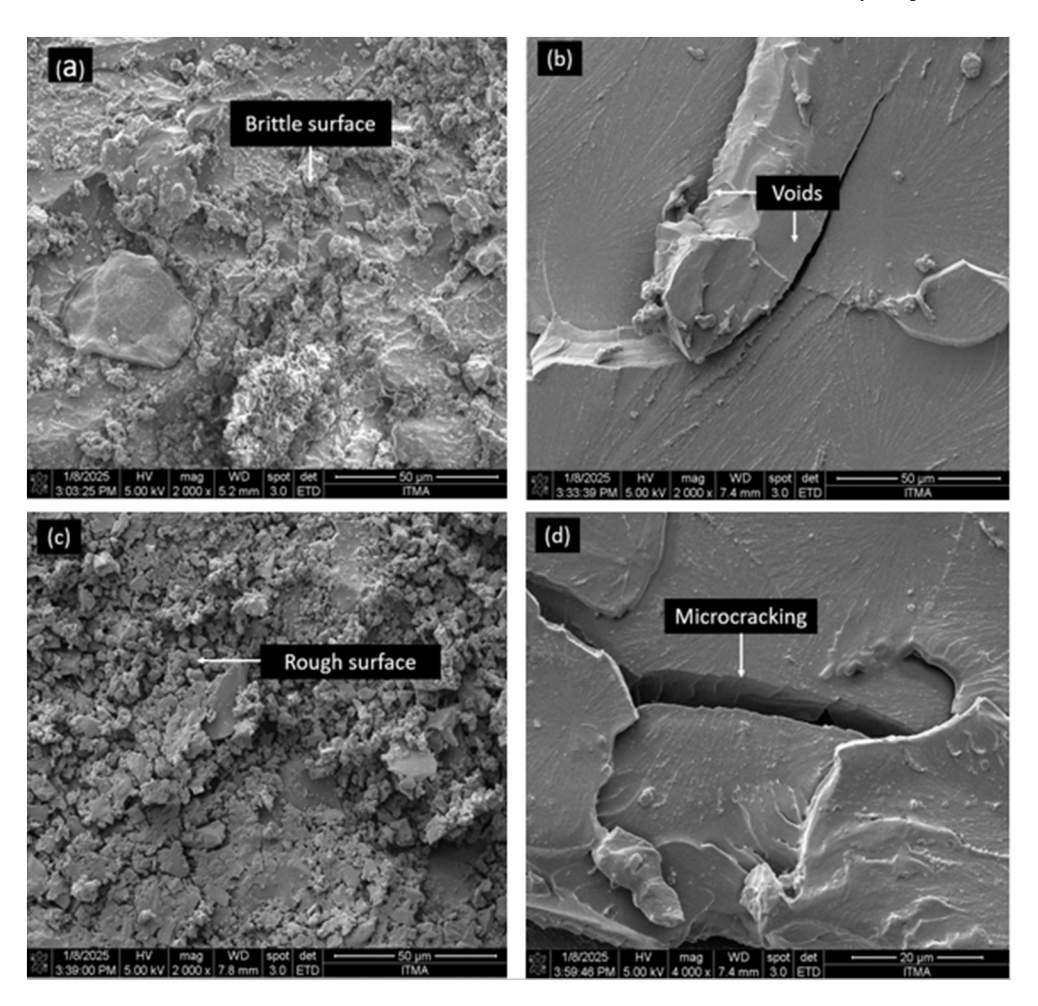


Fig. 10. FE-SEM micrographs of fractured water absorbed bio nanocomposites (a) neat sample (b) 0.1 wt% CNF loading (c) 0.25 wt% CNF loading, (d) 0.5 wt% CNF loading.

lower fiber's concentration were more likely to exhibit fibers debonding and gaps between the fibers and matrix. This result was consistent with the findings of Pothan et al. [87]. Water dissolved in the polymer structure, formed hydrogen bonds with hydrophilic groups in the composites, and was transported and deposited by microcracks on the surface of cellulose fiber-reinforced polymer composites. Both free and bound waters were included in absorbed water; free water traveled freely through voids whereas bound water was restricted to polar polymer groups. Free water attached itself to the hydrophilic groups in the fibers to generate hydrogen bonds [88], which decreased fibermatrix adhesion. As cellulose fibers grew, the matrix surrounding them became brittle and developed microcracks, raising stress in boundary areas. This promoted moisture transport and capillarity, which damaged fibers and caused them to separate from the matrix. As the number of fibers increased, so did the amount of water absorbed. Due to the deterioration of bonding at the fiber-matrix interfaces, two weeks of exposure to moisture resulted in a decrease in hardness and fracture toughness. Nevertheless, it was discovered that impact strength somewhat increased following water absorption. At higher fiber contents, the impact of water absorption on mechanical qualities was more noticeable [89].

Water molecules when penetrating composites through capillary flow via pores and interfaces due to hydrolytic breakdown or microdamage. Absorbed moisture induces notable mechanical and physicochemical alterations that enhance the matrix or compromise the fibermatrix interface through debonding or micro-cracking. In composites utilizing carbon nanoparticles and epoxy resins, moisture absorption is primarily attributed to the epoxy resin, as carbon nanoparticles exhibit

negligible water absorption, illustrated in Fig. 11(b) by delayering from absorbed moisture [90]. The observation was similar to Pittman et al. [91] findings, who also concluded that when water is absorbed, the matrix expands, creating microcracks and delamination at the fibermatrix interface, reducing the overall structural integrity. The elevated cellulose levels in fibers intensify water penetration through microcracks induced by fiber swelling, thereby diminishing composite efficiency. Larger filler dimensions lead to increased composite cracking, which promotes moisture transport, as illustrated in hybrid nano composites in Fig. 12 (d). Higher fiber content correlated with an increased diffusion coefficient, attributable to greater water absorption and cellulose levels. Microcracks at the interface, resulting from fiber swelling, enhance water diffusion, while the capillary mechanism further accelerates water movement through the fiber-matrix interface, elevating diffusivity. Studies indicate that longer fibers exhibit greater swelling and water absorption compared to shorter fibers and particles, owing to their larger size and superior water affinity [92].

The performance of CNF, GNP, and hybrid green epoxy nanocomposites was directly impacted by significant microstructural variations that were identified using Field Emission Scanning Electron Microscopy (FESEM). Higher CNF concentration samples exhibited water absorption-induced fiber-matrix debonding and microcrack development, which resulted in reduced mechanical characteristics. Poor dispersion created micro-voids in GNP-rich samples, which served as stress concentrators and made it easier for moisture to enter. Matrix brittleness and improved capillary-driven moisture transport were the results of the interaction between CNF and epoxy. A modest increase in impact strength was noted, even though water absorption generally

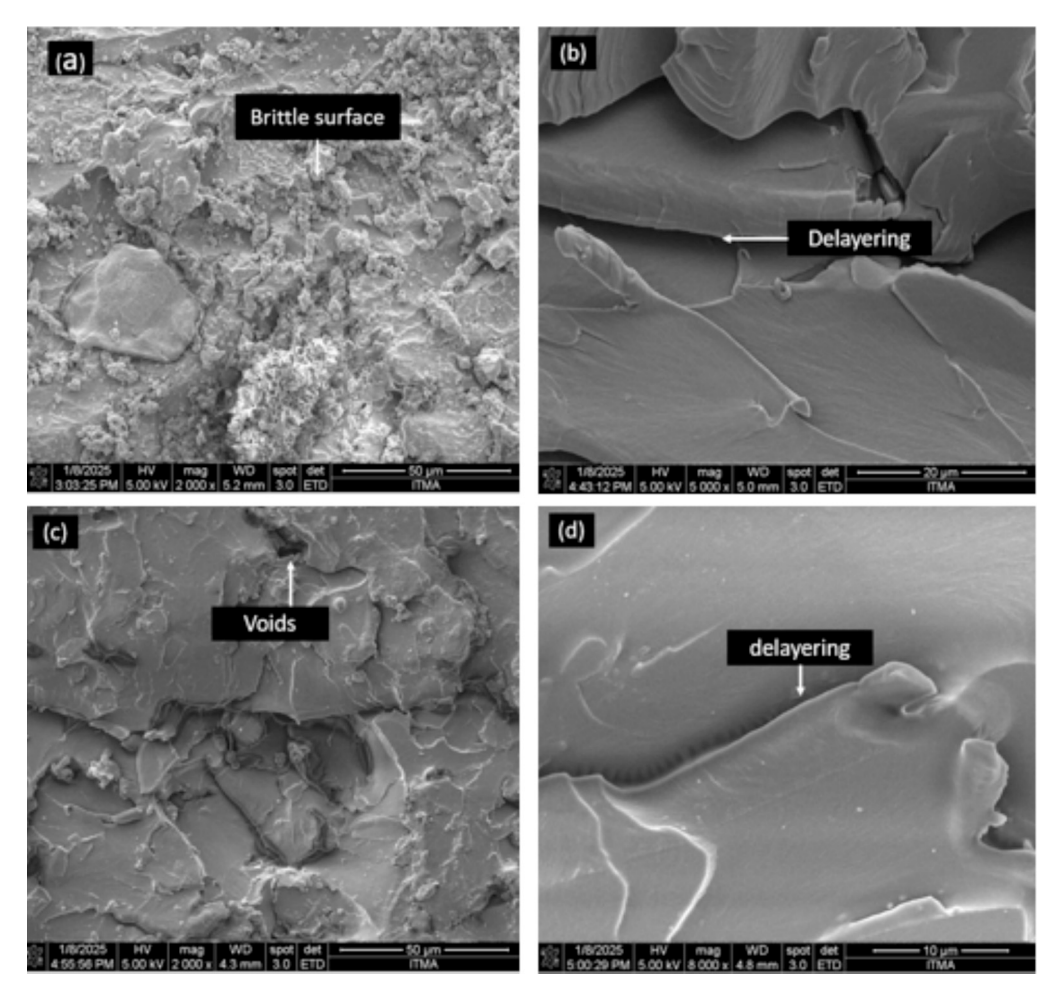


Fig. 11. FE-SEM micrographs of fractured water-absorbed bio nanocomposites (a) neat sample (b) 0.1 wt% GNP loading (c) 0.25 wt% GNP loading, (d) 0.5 wt% GNP loading.

decreased hardness and fracture toughness. Minimizing moisture damage required efficient filler and matrix dispersion and interfacial bonding. While CNF contributed to swelling and density alterations, GNP loadings increased water resistance, but excessive levels resulted in voids. Overall, FESEM demonstrated that the key to maximizing mechanical stability and water resistance in hybrid nanocomposites is filler dispersion and microstructural integrity.

3.6. XRD analysis

Characteristic peaks for polymer composites phases suggested an amorphous structure of all the samples [93]. The peak of CNF was at 15.5° which was in agreement with Nasihin et al. [94]. But the amount of green epoxy that was used overpowered the peak. The peak's intensity is relatively modest because the CNF loading was <1 %. The sonication of GNP and CNF weakens the van der Waal forces of connections between the layers, allowing bio epoxy molecules to intercalate (refer to Fig. 13 (a)). Similarly, sonication and magnetic stirring were used to intercalate nanoparticles that had a strong propensity to bond together in epoxy [95]. As GNP is so thin in comparison to the epoxy matrix structure, it is speculated that it can readily slide and migrate within the wider spaces between the epoxy polymer chains in nanocomposites, thus "filling in" the gaps [96]. Fig. 13 (b) shows XRD graph for neat sample and varying loadings of GNP nanocomposites. There was no obvious diffraction of GNP content at 0.1 wt%, which is believed to be associated with a small amount of consistently dispersed GNP embedded in epoxy matrices [97]. However, at loading 0.5 wt% of GNP and 0.25 wt% of GNP, a visible peak can be seen positioned at 26.31°

and 26.38°.

Fig. 13(c) shows that during sonication, the nanoparticles in the green epoxy matrix separated. Two broader peaks with lower intensities were visible in the nanocomposites. The interaction of two nanoparticles with epoxy molecules, which permitted the molecules to migrate between the layers, were responsible for these peaks. The two unique peaks can be explained by the presence of individual nanoparticles in different places across the system, while lower peak intensities indicate a major disruption in the nanoparticle arrangements. As a result, XRD data results indicate that each nanoparticle was sufficiently dispersed throughout the epoxy system. All nanocomposites XRD graphs show the relative intensity of wider peaks that indicate how the matching nanoparticles were distributed throughout the epoxy system [98].

3.7. Raman analysis

A distinct band was associated to the epoxy resin, which can be seen at $1610~\text{cm}^{-1}$ [99] and at $2900~\text{cm}^{-1}$ [100] in Fig. 14 (a)(i). The Raman signals attributed to nanocellulose groups had been observed. Signal at $380~\text{cm}^{-1}$ was assigned to hydroxyl groups (refer to Fig. 14 (a)(ii), while the peak at $898~\text{cm}^{-1}$ was attributed to C - OH [101]. The bands located in the range of $250\text{-}600~\text{cm}^{-1}$ were due to skeletal-bending modes C-C-C, C-O-C, O-C-C and skeletal stretching modes of C—C and C—O, however only in 0.5 wt% CNF loading the signals were visible and in 0.1 and 0.25 wt% loadings the signals were very weak due to low loadings of CNF [102]. Signal at $1098~\text{cm}^{-1}$ was due to C - O - C ring stretching modes and the β -1,4 glycosidic linkage (C–O–C) stretching modes in cellulose chains [30–32]. The band centered at $1120~\text{cm}^{-1}$ corresponds

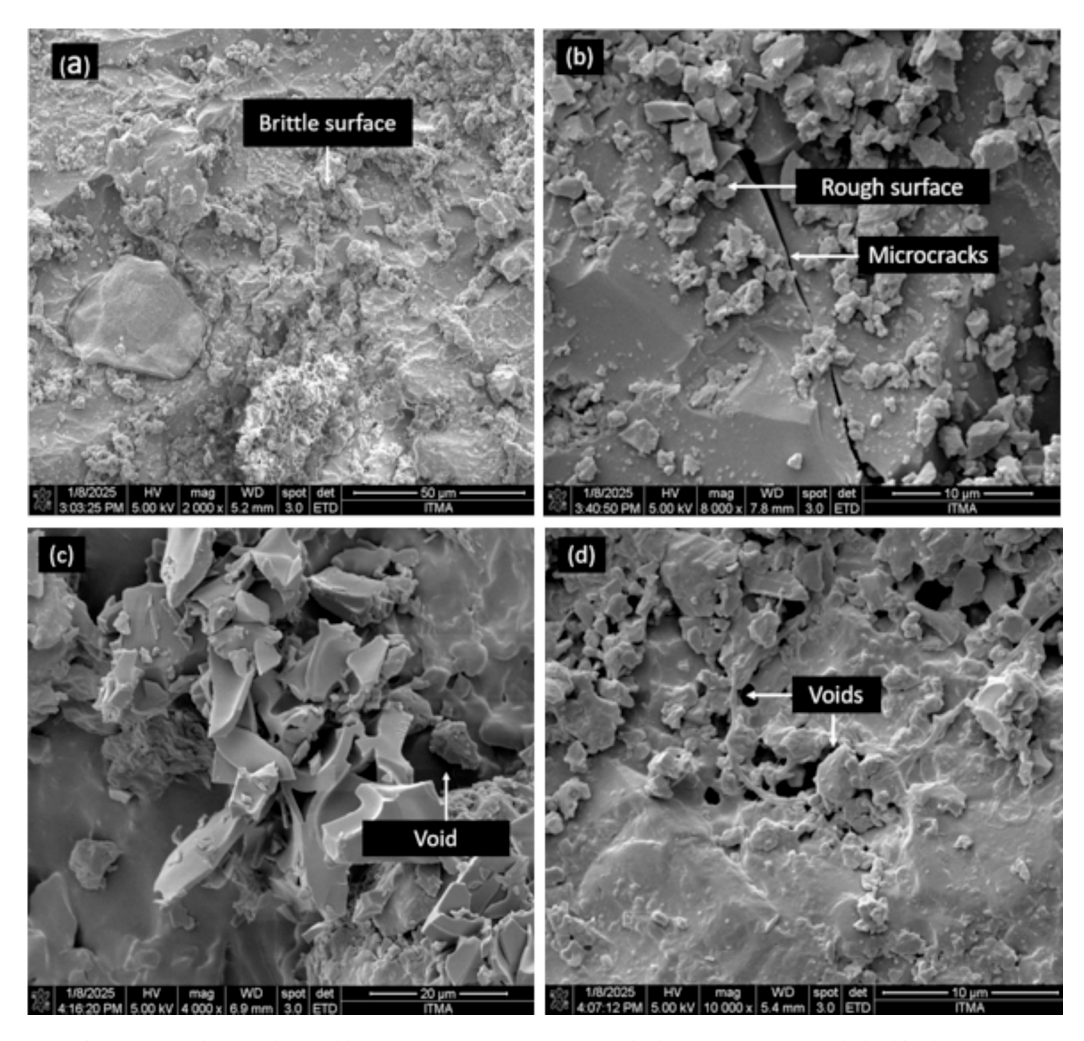


Fig. 12. FE-SEM micrographs of fractured water absorbed bio nanocomposites (a) neat sample (b) 0.1 wt% CNF/GNP hybrid loading (c) 0.25 wt% CNF/GNP loading, (d) 0.5 wt% CNF/GNP loading.

to C - O - C bending in nanocellulose structure [103].

In Raman spectra of water absorbed GNP loaded bio nanocomposites the epoxy resin fingerprint is depicted in Fig. 14 (b), with Raman shift linking to epoxide vibration between 1280 cm⁻¹ and 1230 cm⁻¹. The measurement of epoxide vibration was recorded at 1247 cm⁻¹ [104]. The Raman peak at $826~\text{cm}^{-1}$ was ascribed to -CH wagging vibrations [105]. Additionally, the minor double peak around 1608 cm⁻¹, corresponding to the C=C vibration of the aromatic ring and CHx vibration in the band near 2914 cm⁻¹, affirms the aromatic nature of the bearing aromatic group (where x = functional groups). The G-band, which was the absorption band in the 1590–1620 cm⁻¹ range, was connected to the sp2-hybridized carbon structure's in-plane vibrations. Due to the significant concentration difference between sp3- and sp2-hybridized carbons, the D-band at 1340 cm⁻¹, which was linked to the degree of disorder of the sp3-hybridized carbon structure, was not detectable in GNP/epoxy composites. Both bands were present in the Raman spectra when minutely observed in the spectra [106].

The findings show that the hardener and monomer successfully underwent polymerization to produce a solid epoxy resin. With the leading bands altering wave numbers by $5{\text -}10~{\rm cm}^{-1}$, the spectrum of a green epoxy composite with a reduced concentration of GNP was quite like that of neat epoxy. This change implied that epoxy molecules and GNP interact physically or through Van der Waals forces to generate composites. It emphasized how epoxy and its reinforcement mixed nanofiller GNPs are expected to connect [107]. In hybrid sample the curing reaction can clearly be followed by looking at the characteristic bands of

the epoxide moieties in the region between 1100 and 1450 cm⁻¹ [108]. Assignments of the 380 cm⁻¹ band was particularly important because it was identified as measures of cellulose crystallinity [109] (refer to Fig. 14 (c)).

3.8. Impact test

In this section, various mechanical properties of oil palm cellulose CNF/GNP nanoplatelets reinforced green epoxy hybrid nanocomposites are discussed. To validate the water absorption and density test impact testing was performed (refer to Fig. 15). The Impact test revealed that neat samples did not reveal much difference in the impact test due to its hydrophobic nature. Moreover, the results showed that all the samples showed a reduction in strength that was obvious due to the absorption of water. Only CNF 0.25 wt%, GNP 0.1 wt%, and GNP 0.25 wt% showed a little improvement because of the research carried by Naveen et al. [110] showed that an addition of 0.25 wt% GNP effectively reduced water uptake by closing unoccupied pores within the composite, so enhancing moisture resistance which further increased the impact strength of the sample. GNP with a small size exhibits the best improvement of 75 % for the fracture toughness due to the fine dispersion of small GNP in the epoxy resin [111] GNP also enhances energy absorption by effectively hindering dislocation motion, concentrating stress along interfaces, and promoting microcrack formation, which leads to improved mechanical properties. The microstructural changes, such as swelling and rearrangement of polymer chains due to

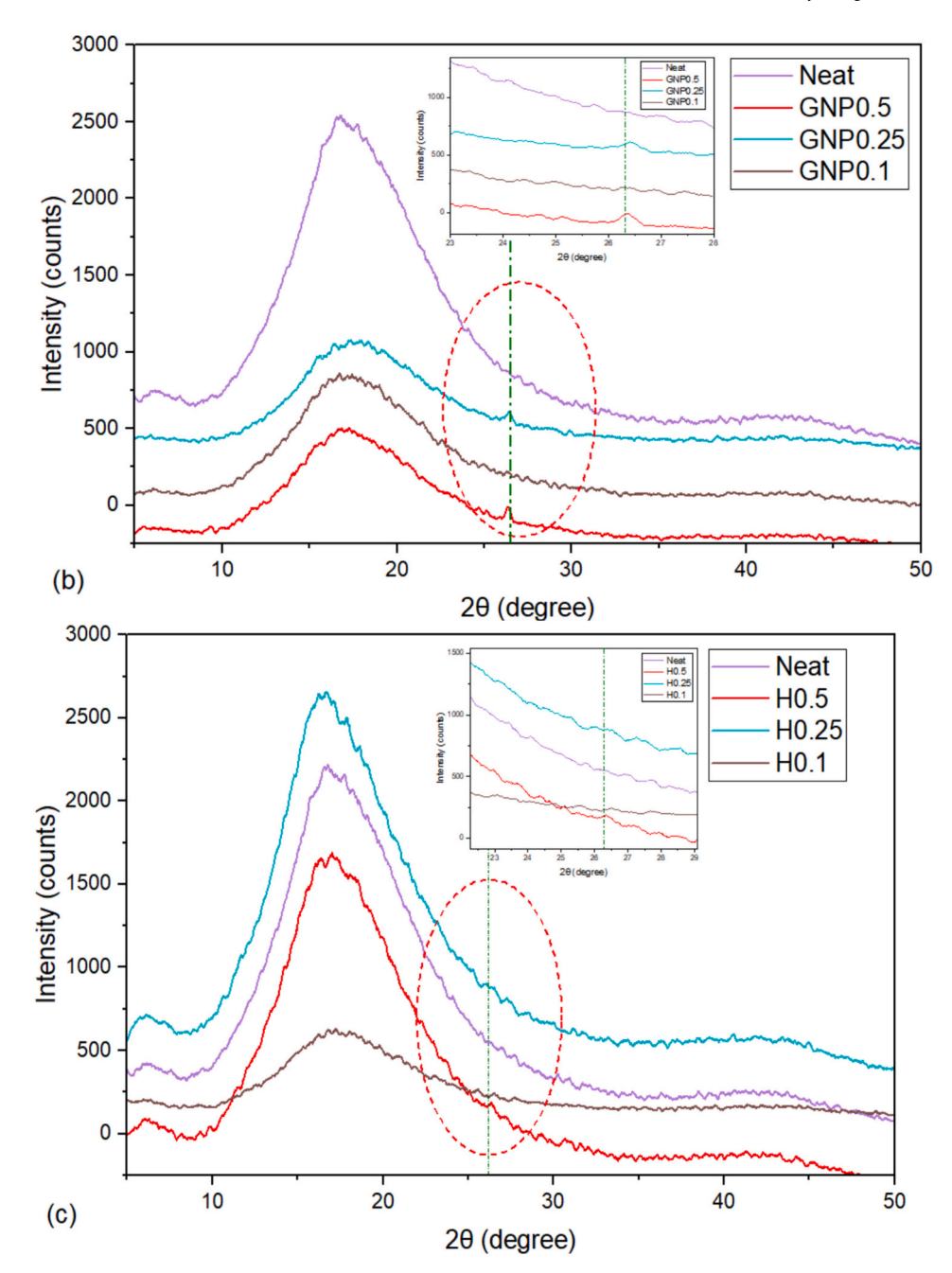


Fig. 13. XRD patterns of water absorbed bio nanocomposites (a) 0.1,0.25 and 0.5 wt% CNF loadings (b) 0.1,0.25 and 0.5 wt% GNP loadings, (c) 0.1,0.25 and 0.5 wt% CNF/GNP hybrid loadings.

water absorption, can also influence the impact resistance. These alterations may lead to a slight increase in impact strength, demonstrating how micro-level changes can affect macro-level performance [112].

In all these cases the weight of epoxy was higher as compared to its other counterparts within the same sets which have water-repelling properties [43]. Also, microstructural alterations in the samples, such as swelling or a little rearrangement of the polymer chains, can be brought about by water absorption. These modifications may lead to a slight rise in impact resistance [113].

In case of hybridization of GNP with CNF, it creates a unique 3D network that further improves the moisture barrier properties of the composites. This network creates a maze-like structure that makes it harder for water molecules to penetrate through the composite and further the complex structure lowers the rate at which moisture can diffuse through the material [114], which was evident in H 0.1 wt%

sample (refer to Fig. 15).

3.9. Hardness test

The water absorbed neat sample showed lower strength as compared to unabsorbed sample as shown in Fig. 16. The hardness of waterabsorbed CNF epoxy composites was significantly influenced by the incorporation of CNF and their interaction with the epoxy matrix. Researchers indicates that the addition of CNF enhanced the mechanical properties of epoxy composites, including hardness, while also improving moisture stability. The presence of CNF reduces water vapor permeability by over 50 %, which contributed to moisture stability and prevents degradation of mechanical properties [115] and was evident in the graph in CNF 0.5 wt% sample. The combination of CNF enhances the mechanical performance, leading to increased hardness [116].

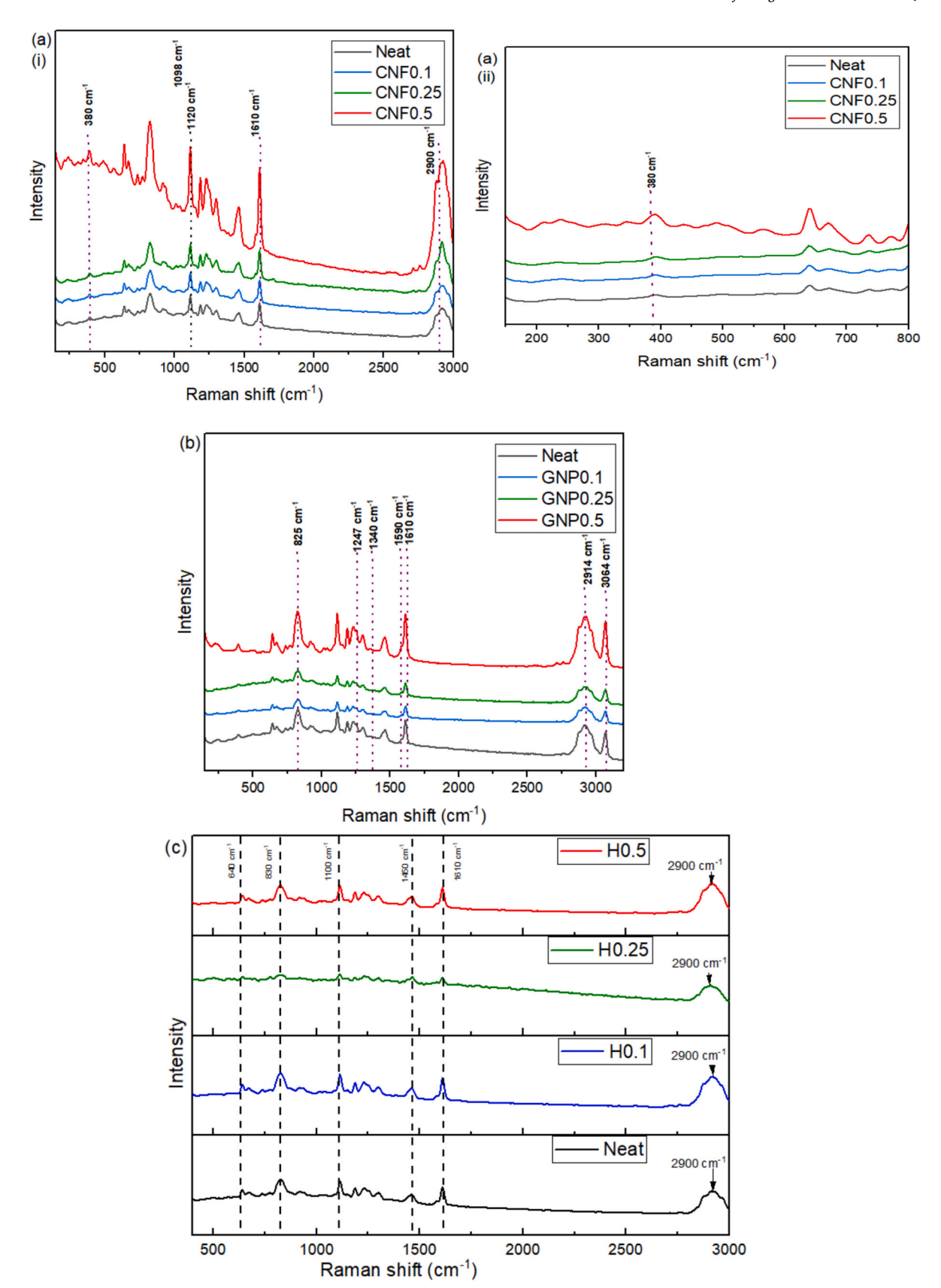


Fig. 14. Raman spectra of water absorbed bio nanocomposites (a) 0.1,0.25 and 0.5 wt% CNF loading (i) unmagnified (ii) magnified (b) 0.1,0.25 and 0.5 wt% GNP loadings, (c) 0.1,0.25 and 0.5 wt% CNF/GNP hybrid loadings.

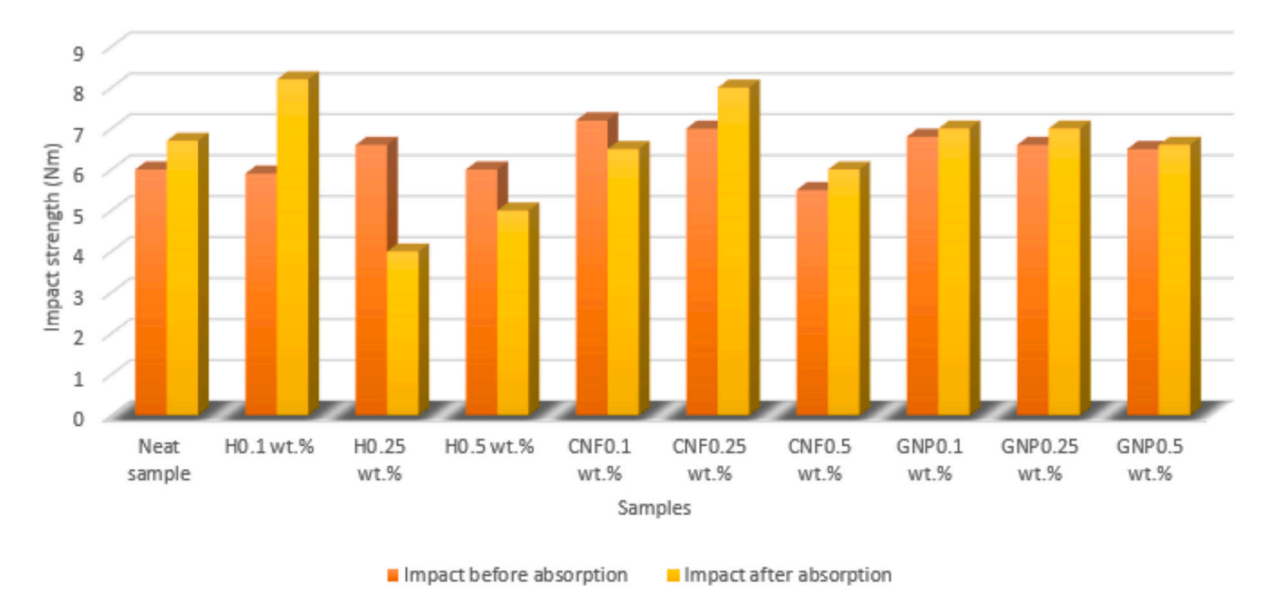


Fig. 15. Impact test data of different CNF, GNP and CNF/GNP hybrid composites loadings.

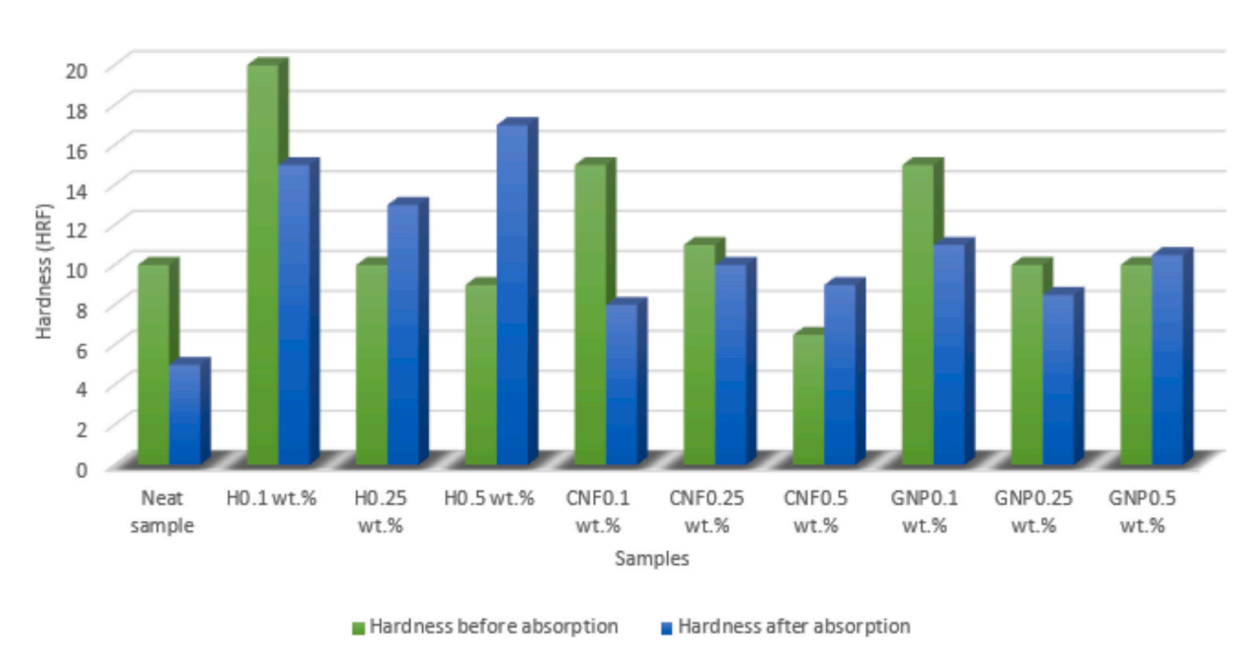


Fig. 16. Rockwell hardness test data of different loadings of CNF, GNP and CNF/GNP hybrid composites.

The water absorption of epoxy composites decreased significantly with GNP addition, from 0.125 % in neat epoxy to 0.067 % at 0.25 wt% GNP [117]. This reduction was attributed to improved interfacial adhesion and pore closure within the nanocomposite structure [110]. Furthermore, the incorporation of GNP into epoxy matrices enhanced the composite's performance, particularly in terms of water resistance and mechanical strength. CNF leads to increased water uptake, while GNP results in reduced absorption [43], as evident in the bar graph of hybrid 0.25 and 0.5 wt% composites, which showed lower water absorption. Micro-tests provide insights into the fundamental properties of CNF and GNP at a small scale, revealing how their interactions affect water absorption and mechanical strength. In contrast, macro performance metrics reflect the overall effectiveness of these composites in practical applications, emphasizing the importance of balancing hydrophilicity and hydrophobicity for optimal material performance. The study illustrates that the combination of CNF and GNP can lead to enhanced properties, making these hybrid nanocomposites suitable for various applications where moisture resistance and mechanical strength

are critical. (refer to Fig. 16)."

4. Conclusions

The study demonstrated that water absorption significantly influences the mechanical and structural integrity of CNF and GNP-reinforced green epoxy composites. While the ideal GNP concentration (e.g., 0.25 wt%) increased impact resistance by lowering pore-related weaknesses, mechanical testing showed decreased strength in all samples. Water exposure results in fiber-matrix debonding and void formation, especially at high CNF and GNP loadings, respectively, according to FESEM analysis. Effective dispersion of the nanofiller is essential for reducing flaws and improving durability, while the contrasting behaviors of hydrophilic CNF and hydrophobic GNP emphasize the necessity of a balanced formulation. The water absorption and density behavior of CNF, GNP, and CNF/GNP hybrid nanocomposites during 15 days of immersion, were investigated. Due to the hydrophilic nature of CNF, readily available hydroxyl groups, and large surface area,

CNF showed substantial water absorption; greater loadings resulted in swelling and enhanced water uptake. In lower concentrations, GNP, which is hydrophobic, decreased water absorption; but, at larger loadings, the existence of voids from poor dispersion boosted water uptake. The hybrid CNF/GNP composites balanced the hydrophilicity of CNF with the barrier qualities of GNP by exhibiting a moderate amount of water absorption. The hydrophobic nature of the neat epoxy samples was confirmed by the small variations in density and water absorption that they displayed the study was in line with the impact test performed which showed a slight increase in the samples with low loadings. The study also showed that, especially in GNP-rich samples, insufficient dispersion of nanomaterials and the existence of micro-voids in the nano composites were important factors in water absorption. GNP loadings decreased water absorption and density however the high GNP loadings lead to void formation which can be seen in FESEM micrographs, while CNF produced swelling in hybrid composites that impacted density. CNF and GNP have opposite trait when it comes in contact of water which was seen in contact angle analysis. Although the loading of GNP was <1 % the XRD graph showed the presence of GNP in the form of a small peak. The also study reports a 46.6 % increase in hardness for waterabsorbed hybrid nanocomposites, indicating a significant enhancement in mechanical properties due to the incorporation of GNP and CNF. The thermal conductivity values of the composites were reported to be between 10 and 30 W/m•K, which supports efficient heat dissipation and indicates a favorable thermal management capability for applications in electronics. The results highlight how important interfacial bonding and nanomaterial dispersion are for maximizing water resistance and preserving the structural integrity of nanocomposites. These observations are helpful in the development of composites that meet the requirements of mechanical stability and moisture resistance.

While this study provided valuable insights into the properties of CNF/GNP-reinforced green epoxy nanocomposites, several challenges remain. Addressing issues related to water absorption, filler content, dispersion, environmental stability, and manufacturing scalability will be essential for advancing the development and application of these sustainable materials in various industries., it should be noted that this study only examined a low range of water-absorbed GNP and CNF loadings in bio-based epoxy, and it only included physical, mechanical, and morphological characteristics. Future studies can examine how these results can be applied more broadly to various green polymer matrices, with an emphasis on electrical characteristics, chemical stability, chemical resistance, environmental performance, and the commercial application of green nanocomposites.

CRediT authorship contribution statement

J. Yusuf: Writing – original draft. S.M. Sapuan: Supervision. Umer Rashid: Supervision. R.A. Ilyas: Supervision. M.R. Hassan: Supervision.

Declaration of competing interest

The authors declare the following financial interests/personal relationships which may be considered as potential competing interests: Prof. Ir. Dr. Mohd. Sapuan Bin Salit reports was provided by Putra Malaysia University. If there are other authors, they declare that they have no known competing financial interests or personal relationships that could have appeared to influence the work reported in this paper.

Acknowledgments

The authors wish to thank Puncak RM Sdn. Bhd. Terengganu, Malaysia for giving research grant, under project number V26000. The authors are also thankful to Universiti Pura Malaysia (UPM) for providing Putra IPS vote number 9742900. The authors are grateful for the financial support given by The Ministry of Higher Education

Malaysia (MOHE) under the Higher Institution Centre of Excellence (HICoE2.0/6369123) at Institute of Tropical Forestry and Forest Products. The authors want to thank (MoHE) for providing the financial support through Malaysia International Scholarship (MIS).

Data availability

Data will be made available on request.

References

- [1] A. Ahmad, M.H. Sutanto, I.S.H. Harahap, M.A.M. Al-Bared, M.A. Khan, Feasibility of Demolished Concrete and Scraped Tires in Peat Stabilization – A Review on the Sustainable approach in Stabilization, Second Int. sustain. Resil. Conf. Technol. Innov. Build. Des, IEEE 2020 (2020) 1–5, https://doi.org/10.1109/ IEEECONF51154.2020.9319953.
- [2] W. Tang, L. Luo, Y. Chen, J. Li, Y. Dai, Y. Xie, et al., Noble-metal-free bi-OZIS nanohybrids for sacrificial-agent-free photocatalytic water splitting: with long-lived photogenerated electrons, Sep. Purif. Technol. 357 (2025) 130047, https://doi.org/10.1016/j.seppur.2024.130047.
- [3] Z. Candan, A. Tozluoglu, O. Gonultas, M. Yildirim, H. Fidan, M.H. Alma, et al., in: S.M. Sapuan, M.N.F. Norrrahim, R.A. Ilyas, Soutis, CBT-IA of N and IN (Eds.), Nanocellulose: Sustainable biomaterial for developing novel adhesives and composites, Elsevier, 2022, pp. 49–137, https://doi.org/10.1016/B978-0-323-89909-3.00015-8, editors. Ind. Appl. Nanocellulose Its Nanocomposites.
- [4] A. Nurnadia, R.A. Roshafima, A.L. Nur Shazwani, A. Hafizah, Z W Yunus WM, Fatehah R., Effect of Silane treatment on rise straw/high density polyethylene biocomposites, J Nat Fibre Polym Compos 2 (2023) 2821–3289.
- [5] M.Z. Zainudin, M.R. Mansor, M.B. Ali, Y. Jameel, S.M. Sapuan, Effect of varying fibre loadings on the impact performance of Kenaf and Coir effect of varying fibre loadings on the impact performance of Kenaf and Coir reinforced Bioepoxy composites, 2023.
- [6] H. Yang, Y. Duan, Y. Dai, Y. Chen, Y. Xie, G. Zhang, et al., CeO2-x decorated CoFe-LDH on nickel foam with moderated oxygen vacancies for the oxygen evolution reaction. Colloids Surf. A Physicochem. Eng. Asp. 709 (2025) 136055.
- [7] N.K. Arora, I. Mishra, United Nations sustainable development goals 2030 and environmental sustainability: race against time, Environ. Sustain. 2 (2019) 339–342, https://doi.org/10.1007/s42398-019-00092-y.
- [8] D. Trache, M.H. Hussin, N. Brosse, Recent trends in preparation, characterization and applications of nanocellulose, Front. Chem. 8 (2020) 594379.
- [9] M.R.M. Asyraf, M. Rafidah, Mechanical and thermal performance of sugar palm fibre- thermoset polymer composites: a short review 1 (2022) 157–180.
- [10] L. Li, B. Zhou, G. Han, Y. Feng, C. He, F. Su, et al., Understanding the effect of interfacial engineering on interfacial thermal resistance in nacre-like cellulose nanofiber/graphene film, Compos. Sci. Technol. 197 (2020) 108229, https://doi. org/10.1016/j.compscitech.2020.108229.
- [11] F. Norrrahim, S.M. Shakrin N.N. MN, A. Shukor MF, N.N. Shukor, S.A. Junaidi NS, V.F. Knight, et al., Advancements in functionalized Nanocellulose and its composites for biomedical applications, J Nat Fibre Polym Compos 2 (2023) 2821–3289.
- [12] G. Yang, H. Kong, Y. Chen, B. Liu, D. Zhu, L. Guo, et al., Recent advances in the hybridization of cellulose and carbon nanomaterials: interactions, structural design, functional tailoring, and applications, Carbohydr. Polym. 279 (2022) 118947. https://doi.org/10.1016/j.carbpol.2021.118947.
- [13] S. Radhakrishnan, R. Mishra, V. Dhyani, S.P. Dwivedi, S.D. Sadhu, P. Gupta, et al., Studies on water uptake behavior and mechanical performance of bio-wastagereinforced bio composites for improved sustainability, Biomass Convers. Biorefinery (2024), https://doi.org/10.1007/s13399-024-05449-w.
- [14] M.D.R. Islam, S. Ismail, Fabrication and optimization of reinforced polyester composite using banana fiber, eggshell and rice husk, J Nat Fibre Polym Compos 2 (2023) 2821–3289.
- [15] S. Han, P. Wang, Y. Zhou, Q. Meng, M. Aakyiir, J. Ma, Flexible, mechanically robust, multifunctional and sustainable cellulose/graphene nanocomposite films for wearable human-motion monitoring, Compos. Sci. Technol. 230 (2022) 109451 https://doi.org/10.1016/j.compositech.2022.109451
- 109451, https://doi.org/10.1016/j.compscitech.2022.109451.
 [16] J. Li, F. Yang, D. Liu, S. Han, J. Li, G. Sui, Graphene composite paper synergized with micro/nanocellulose-fiber and silk fibroin for flexible strain sensor, Int. J. Biol. Macromol. 240 (2023) 124439, https://doi.org/10.1016/j.ijbiomac.2023.124439.
- [17] J. Yusuf, S.M. Sapuan, M.A. Ansari, V.U. Siddiqui, T. Jamal, R.A. Ilyas, et al., Exploring nanocellulose frontiers: a comprehensive review of its extraction, properties, and pioneering applications in the automotive and biomedical industries, Int. J. Biol. Macromol. 255 (2024), https://doi.org/10.1016/j. iibiomac.2023.128121, 128–121.
- [18] U.R. Hashim, A. Jumahat, Improved tensile and fracture toughness properties of graphene nanoplatelets filled epoxy polymer via solvent compounding shear milling method, Mater. Res. Express 6 (025303) (2018) 025303, https://doi.org/ 10.1088/2053-1591/aaeaf0.
- [19] U. Kilic, M.M. Sherif, O.E. Ozbulut, Tensile properties of graphene nanoplatelets/epoxy composites fabricated by various dispersion techniques, Polym. Test. 76 (2019) 181–191, https://doi.org/10.1016/j.polymertesting.2019.03.028.

- [20] L. Jarosinski, A. Rybak, K. Gaska, G. Kmita, R. Porebska, C. Kapusta, Enhanced thermal conductivity of graphene nanoplatelets epoxy composites, Mater. Sci. Pol. 35 (2017) 382–389, https://doi.org/10.1515/msp-2017-0028.
- [21] M. Asim, M.T. Paridah, M. Chandrasekar, R.M. Shahroze, M. Jawaid, M. Nasir, et al., Thermal stability of natural fibers and their polymer composites, Iran. Polym. J. 29 (2020) 625–648, https://doi.org/10.1007/s13726-020-00824-6.
- [22] M. Ababu, E. Husen, B. Awraris, N. Bashawal, Review of the applications and properties of bamboo Fiber reinforced composite materials, Glob Sci J 9 (2021) 1196–1204, https://doi.org/10.11216/gsj.2021.03.49470.
- [23] K. Bilisik, M. Akter, Graphene nanoplatelets/epoxy nanocomposites: a review on functionalization, characterization techniques, properties, and applications, J. Reinf. Plast. Compos. 41 (2022) 99–129, https://doi.org/10.1177/ 07316844211049277.
- [24] S. Yue, H. Tong, Z. Gao, W. Bai, L. Lu, J. Wang, et al., Fabrication of flexible nanoporous nitrogen-doped graphene film for high-performance supercapacitors, J. Solid State Electrochem. 21 (2017) 1653–1663, https://doi.org/10.1007/ s10008-017-3538-v.
- [25] X. Tang, D. Zeng, D. Chen, W. Guo, J. Fu, L. Zou, Porous silicon particles embedded in N-doped graphene and carbon nanotube framework for highperformance lithium-ion batteries, J. Alloys Compd. 927 (2022) 167055, https:// doi.org/10.1016/j.jallcom.2022.167055.
- [26] P. Jindal, P. Sharma, M. Kundu, S. Singh, D. Kumar, V. Jit, et al., Computational fluid dynamics (CFD) analysis of graphene nanoplatelets for the cooling of a multiple tier Li-ion battery pack, Therm. Sci. Eng. Prog. 31 (2022) 101282, https://doi.org/10.1016/j.tsep.2022.101282.
- [27] C. Deng, J. Jiang, F. Liu, L. Fang, J. Wang, D. Li, et al., Influence of graphene oxide coatings on carbon fiber by ultrasonically assisted electrophoretic deposition on its composite interfacial property, Surf. Coat. Technol. 272 (2015) 176–181, https://doi.org/10.1016/j.surfcoat.2015.04.008.
- [28] L. Yue, G. Pircheraghi, S.A. Monemian, I. Manas-Zloczower, Epoxy composites with carbon nanotubes and graphene nanoplatelets – dispersion and synergy effects, Carbon N Y 78 (2014) 268–278, https://doi.org/10.1016/j. carbon 2014 07 003
- [29] M.T. Le, S.C. Huang, Thermal and mechanical behavior of hybrid polymer nanocomposite reinforced with graphene nanoplatelets, Materials (Basel) 8 (2015) 5526–5536, https://doi.org/10.3390/ma8085262.
- [30] R.M. Nauman Javed, A. Al-Othman, M. Tawalbeh, A.G. Olabi, Recent developments in graphene and graphene oxide materials for polymer electrolyte membrane fuel cells applications, Renew. Sust. Energ. Rev. 168 (2022) 112836, https://doi.org/10.1016/j.rser.2022.112836.
- [31] D. Trache, A.F. Tarchoun, A. Abdelaziz, W. Bessa, S. Thakur, M.H. Hussin, et al., A comprehensive review on processing, characteristics, and applications of cellulose nanofibrils/graphene hybrid-based nanocomposites: toward a synergy between two-star nanomaterials, Int. J. Biol. Macromol. 268 (2024) 131633, https://doi.org/10.1016/j.ijbiomac.2024.131633.
- [32] J. Yusuf, A.H.M. Firdaus, S.M. Sapuan, U. Rashid, R.A. Ilyas, M.R. Hassan, et al., Nanocellulose-graphene hybrid composites: fabrication, characterization, applications and environmental impact, Int. J. Biol. Macromol. 282 (2024) 137244. https://doi.org/10.1016/j.jibiomac.2024.137244.
- 137244, https://doi.org/10.1016/j.ijbiomac.2024.137244.

 [33] Z.G. Mohammadsalih, N.S. Sadeq, Structure and properties of polystyrene/graphene oxide nanocomposites, Fullerenes Nanotubes Carbon Nanostruct. 30 (2022) 373–384, https://doi.org/10.1080/1536383X.2021.1943367.
- [34] Y. Wei, X. Hu, Q. Jiang, Z. Sun, P. Wang, Y. Qiu, et al., Influence of graphene oxide with different oxidation levels on the properties of epoxy composites, Compos. Sci. Technol. 161 (2018), https://doi.org/10.1016/j.compscitech.2018.04.007.
- [35] J. Yusuf, S.M. Sapuan, U. Rashid, R.A. Ilyas, M.R. Hassan, Thermal, mechanical, t <scp>hermo-mechanical</scp> and morphological properties of graphene nanoplatelets reinforced green epoxy nanocomposites, Polym. Compos. 45 (2024) 1998–2011. https://doi.org/10.1002/pc.27900.
- [36] A. Razzak, F. Mannai, R. Khiari, Y. Moussaoui, N. Belgacem M., Cellulose fibre from Schinus molle and its characterization, J Renew Mater 10 (2022) 2593–2606, https://doi.org/10.32604/jrm.2022.021706.
- [37] S. Ma, T. Li, X. Liu, J. Zhu, Research progress on bio-based thermosetting resins, Polym. Int. 65 (2016) 164–173, https://doi.org/10.1002/pi.5027.
- [38] P. Jojibabu, Y.X. Zhang, B.G. Prusty, A review of research advances in epoxy-based nanocomposites as adhesive materials, Int. J. Adhes. Adhes. 96 (2020) 102454, https://doi.org/10.1016/j.jiadhadh.2019.102454.
- [39] S. Liu, V.S. Chevali, Z. Xu, D. Hui, H. Wang, A review of extending performance of epoxy resins using carbon nanomaterials, Compos. Part B Eng. 136 (2018) 197–214, https://doi.org/10.1016/j.compositesb.2017.08.020.
- [40] H. Khoramishad, M. Khakzad, Toughening epoxy adhesives with multi-walled carbon nanotubes, J. Adhes. 94 (2018) 15–29, https://doi.org/10.1080/ 00218464.2016.1224184.
- [41] J. Wu, C. Li, B. Hailatihan, L. Mi, Y. Baheti, Y. Yan, Effect of the addition of thermoplastic resin and composite on mechanical and thermal properties of epoxy resin, Polymers (Basel) 14 (2022), https://doi.org/10.3390/ polym14061087
- [42] B. Wang, D. Li, G. Xian, C. Li, Effect of immersion in water or alkali solution on the structures and properties of epoxy resin, Polymers 13 (2021), https://doi.org/ 10.3300/colum13121002
- [43] N. Kong, N.Z. Khalil, H. Fricke, Moisture absorption behavior and adhesion properties of gnp/epoxy nanocomposite adhesives, Polymers (Basel) 13 (2021) 1–17, https://doi.org/10.3390/polym13111850.
- [44] G. de A.S. da Silva, J.R.M. d'Almeida, D.C.T. Cardoso, Investigation on moisture absorption behavior on GFRP and neat epoxy systems in hygrothermal salt fog

- aging, Compos. Part B Eng. 272 (2024) 11–13, https://doi.org/10.1016/j.
- [45] Amin KF, Asrafuzzaman, Nahin AM, Hoque ME. Polymer nanocomposites for adhesives and coatings. In: Hoque ME, Ramar K, Sharif ABT-APN, editors. Woodhead Publ. Mater., Woodhead Publishing; 2022, p. 235–65. doi:doi: https://doi.org/10.1016/B978-0-12-824492-0.00014-3.
- [46] N. Farzanehfar, A. Taheri, F. Rafiemanzelat, O.M. Jazani, High-performance epoxy nanocomposite adhesives with enhanced mechanical, thermal and adhesion properties based on new nanoscale ionic materials, Chem. Eng. J. 471 (2023) 144428, https://doi.org/10.1016/j.cej.2023.144428.
- [47] H. Khoramishad, O. Alizadeh, L.F.M. da Silva, Effect of multi-walled carbon nanotubes and silicon carbide nanoparticles on the deleterious influence of water absorption in adhesively bonded joints, J. Adhes. Sci. Technol. 32 (2018) 1795–1808, https://doi.org/10.1080/01694243.2018.1447295.
- [48] M.A.A. Ahmad, M.J.M. Ridzuan, M.S. Abdul Majid, S.M. Sapuan, A.B. Shahriman, F. Mat, Effect of water absorption on graphene Nanoplatelet and multiwalled carbon nanotubes-impregnated glass fibre-reinforced epoxy composites, J. Inorg. Organomet. Polym. Mater. 33 (2023) 1802–1816, https://doi.org/10.1007/s10904-023-02610-2
- [49] A. Oun, A. Manalo, O. Alajarmeh, R. Abousnina, A. Gerdes, Long-term water absorption of hybrid flax fibre-reinforced epoxy composites with graphene and its influence on mechanical properties, Polymers (Basel) 14 (2022) 3679, https:// doi.org/10.3390/polym14173679.
- [50] M. Shettar, S. Kowshik, P. Hiremath, S. Sharma, Water sorption-desorption-resorption effects on mechanical properties of epoxy-nanoclay nanocomposites, Int J Automot Mech Eng 19 (2022) 9478–9486.
- [51] B. Venkatesan, S. Ramasamy, J. Duraivelu, J. Thomas, K. Thangappan, S. Venkatesan, et al., Mechanical, thermal conductivity and water absorption of hybrid Nano-silica coir Fiber Mat reinforced epoxy resin composites, Mater Plast 59 (2022) 194–203.
- [52] B. Singh, A. Mohanty, Study of water absorption properties of annealed Nanodiamond/epoxy nanocomposites, J. Surf. Sci. Technol. 37 (2021) 15–21, https://doi.org/10.18311/jsst/2021/25380.
- [53] V. Prasad, K. Sekar, M.A. Joseph, Mechanical and water absorption properties of nano TiO2 coated flax fibre epoxy composites, Constr. Build. Mater. 284 (2021) 122803
- [54] A. Uthaman, H.M. Lal, C. Li, G. Xian, S. Thomas, Mechanical and water uptake properties of epoxy nanocomposites with surfactant-modified functionalized multiwalled carbon nanotubes, Nanomaterials 11 (2021) 1–15, https://doi.org/ 10.3390/nano11051234.
- [55] Chandel, PS, Gupta, NK, Tyagi, YK, Jha, K. Experimental investigation of water absorptions and Charpy test of epoxy composite immersed in different aqueous medium. Recent trends Ind. prod. eng. sel. proc. ICAST 2020. Springer; 2022, p. 79–92.
- [56] J. Yusuf, S.M. Sapuan, U. Rashid, R.A. Ilyas, M.R. Hassan, Thermal, mechanical, and morphological properties of oil palm cellulose nanofibril reinforced green epoxy nanocomposites, Int. J. Biol. Macromol. 278 (2024) 134421, https://doi.org/10.1016/j.ijbiomac.2024.134421.
- [57] X. Guo, Y. Wu, X. Xie, Water vapor sorption properties of cellulose nanocrystals and nanofibers using dynamic vapor sorption apparatus, Sci. Rep. 7 (2017) 14207.
- [58] S.S. Rana, M.K. Gupta, Variations in the mechanical properties of bionanocomposites by water absorption, Proc. Inst. Mech. Eng. Part L J. Mater. Des. Appl. 235 (2021) 1655–1664, https://doi.org/10.1177/ 1464420721090644
- [59] J. Li, L. Wei, W. Leng, J.F. Hunt, Z. Cai, Fabrication and characterization of cellulose nanofibrils/epoxy nanocomposite foam, J. Mater. Sci. 53 (2018) 4949–4960, https://doi.org/10.1007/s10853-017-1652-y.
- [60] A.H. Bedane, M. Eić, M. Farmahini-Farahani, H. Xiao, Theoretical modeling of water vapor transport in cellulose-based materials, Cellulose 23 (2016) 1537–1552
- [61] L. Solhi, V. Guccini, K. Heise, I. Solala, E. Niinivaara, W. Xu, et al., Understanding nanocellulose-water interactions: turning a detriment into an asset, Chem. Rev. 123 (2023) 1925–2015.
- [62] Y. Dan-mallam, T.W. Hong, M.S. Abdul Majid, Mechanical characterization and water absorption behaviour of interwoven kenaf/PET fibre reinforced epoxy hybrid composite, Int J Polym Sci 2015 (2015) 371958.
- [63] A. Namdev, R. Purohit, A. Telang, A. Kumar, Fabrication and different characterization of graphene Nano platelets reinforced epoxy Nano composites, Arch. Metall. Mater. 68 (2023) 823–832, https://doi.org/10.24425/ amm.2023.143675.
- [64] P. Jojibabu, G.D.J. Ram, A.P. Deshpande, S.R. Bakshi, Effect of carbon nano-filler addition on the degradation of epoxy adhesive joints subjected to hygrothermal aging, Polym. Degrad. Stab. 140 (2017) 84–94.
- [65] S. Pandiyan, J. Krajniak, G. Samaey, D. Roose, E. Nies, A molecular dynamics study of water transport inside an epoxy polymer matrix, Comput. Mater. Sci. 106 (2015) 29–37.
- [66] P.S. Yadav, R. Purohit, A. Namdev, Physical and mechanical properties of hybrid composites using Kevlar fibre and nano-SiO2, Adv. Mater. Process. Technol. 8 (2022) 2057–2069.
- [67] T.C. Mokhena, M.J. Mochane, A. Mtibe, S. Sigonya, B. Ntsendwana, E.G. Masibi, et al., Recent advances on nanocellulose-graphene oxide composites: a review, Cellulose 31 (12) (2024) 1–43.
- 68] A. Białkowska, M. Bakar, W. Kucharczyk, I. Zarzyka, Hybrid epoxy nanocomposites: improvement in mechanical properties and toughening

- mechanisms—a review, Polymers (Basel) 15 (2023), https://doi.org/10.3390/polym15061398
- [69] J.-H. Lee, Y.-S. Kim, H.-J. Ru, S.-Y. Lee, S.-J. Park, Highly flexible fabrics/epoxy composites with hybrid carbon Nanofillers for absorption-dominated electromagnetic interference shielding, Nano-Micro Lett 14 (2022) 188, https://doi.org/10.1007/s40820-022-00926-1.
- [70] C. Zou, J.C. Fothergill, S.W. Rowe, The effect of water absorption on the dielectric properties of epoxy nanocomposites, IEEE Trans. Dielectr. Electr. Insul. 15 (2008) 106–117.
- [71] V. Calvo, C. Martínez-Barón, L. Fuentes, W.K. Maser, A.M. Benito, J.M. González-Domínguez, Nanocellulose: the ultimate green aqueous dispersant for nanomaterials, Polymers (Basel) 16 (2024) 1664.
- [72] K.P. Srinivasa Perumal, L. Selvarajan, P. Mathan Kumar, S. Shriguppikar, Enhancing mechanical and morphological properties of glass fiber reinforced epoxy polymer composites through rutile nanoparticle incorporation, Prog. Addit. Manuf. 10 (1) (2024) 1–18.
- [73] Y. Zhong, A. Zhou, J. Du, S. Zhan, Dependence of clay–water contact angle on surface charge and ambient temperature: a study from molecular dynamics perspective, J. Mol. Liq. 415 (2024) 126258, https://doi.org/10.1016/j. mollia.2024.126258.
- [74] A. Moudood, A. Rahman, A. Öchsner, M. Islam, G. Francucci, Flax fiber and its composites: an overview of water and moisture absorption impact on their performance, J. Reinf. Plast. Compos. 38 (2019) 323–339.
- [75] A.S. Sridhar, L.A. Berglund, J. Wohlert, Wetting of native and acetylated cellulose by water and organic liquids from atomistic simulations, Cellulose 30 (2023) 8089–8106
- [76] S. Wang, M. Cao, G. Wang, F. Cong, H. Xue, Q. Meng, et al., Effect of graphene nanoplatelets on water absorption and impact resistance of fibre-metal laminates under varying environmental conditions, Compos. Struct. 281 (2022) 114977, https://doi.org/10.1016/j.compstruct.2021.114977.
- [77] S. Kashi, R.K. Gupta, T. Baum, N. Kao, S.N. Bhattacharya, Phase transition and anomalous rheological behaviour of polylactide/graphene nanocomposites, Compos. Part B Eng. 135 (2018) 25–34, https://doi.org/10.1016/j. compositesb.2017.10.002.
- [78] S. Peretz Damari, L. Cullari, R. Nadiv, Y. Nir, D. Laredo, J. Grunlan, et al., Graphene-induced enhancement of water vapor barrier in polymer nanocomposites, Compos. Part B Eng. 134 (2018) 218–224, https://doi.org/ 10.1016/j.compositesb.2017.09.056.
- [79] S.B. Smedley, Y. Chang, C. Bae, M.A. Hickner, Measuring water hydrogen bonding distributions in proton exchange membranes using linear Fourier transform infrared spectroscopy, Solid State Ionics 275 (2015) 66–70.
- [80] J. Yusuf, S.M. Sapuan, U. Rashid, R.A. Ilyas, M.R. Hassan, Thermal, mechanical, and morphological properties of oil palm cellulose nanofibril reinforced green epoxy nanocomposites, Int. J. Biol. Macromol. 278 (2024) 134421, https://doi.org/10.1016/i.jibjomac.2024.134421.
- [81] X. Guo, Y. Wu, Characterizing molecular structure of water adsorbed by cellulose nanofiber film using in situ Micro-FTIR spectroscopy, J. Wood Chem. Technol. 37 (2017) 383–392. https://doi.org/10.1080/02773813.2017.1306078.
- [82] P.-Y. Kuo, N. Yan, M. Sain, Influence of cellulose nanofibers on the curing behavior of epoxy/amine systems, Eur. Polym. J. 49 (2013) 3778–3787, https://doi.org/10.1016/j.eurpolymj.2013.08.022.
- [83] M. Nuruddin, M. Hosur, R. Gupta, G. Hosur, A. Tcherbi-Narteh, S. Jeelani, Cellulose nanofibers-graphene Nanoplatelets hybrids Nanofillers as highperformance multifunctional reinforcements in epoxy composites, Polym. Polym. Compos. 25 (2017) 273–284, https://doi.org/10.1177/096739111702500404.
- [84] M. Mohammed, R. Rahman, A.M. Mohammed, T. Adam, B.O. Betar, A.F. Osman, et al., Surface treatment to improve water repellence and compatibility of natural fiber with polymer matrix: recent advancement, Polym. Test. 115 (2022) 107707, https://doi.org/10.1016/j.polymertesting.2022.107707.
- [85] R.D. Guha, E.O. Danilov, K. Berkowitz, O. Oluwajire, L.R. Grace, Consequences of humidity cycling on the moisture absorption characteristics of epoxy resins with different network architectures, ACS Appl Polym Mater 5 (2023) 400–411, https://doi.org/10.1021/acsapm.2c01570.
- [86] Y. Qing, R. Sabo, Y. Wu, Z. Cai, High-performance cellulose nanofibril composite films, Bioresour 7 (Number 3) (2012) 3064–3075, 2012;7:3064–75.
- [87] L.A. Pothan, Z. Oommen, S. Thomas, Dynamic mechanical analysis of banana fiber reinforced polyester composites, Compos. Sci. Technol. 63 (2003) 283–293, https://doi.org/10.1016/S0266-3538(02)00254-3.
- [88] S. Lim, H.K. Shon, in: S. Sarp, N. Hilal (Eds.), Characterization of membranes for membrane-based salinity-gradient processes, Elsevier, 2018, pp. 125–154, https://doi.org/10.1016/B978-0-444-63961-5.00004-3, editors. In: Sarp S, Hilal NBT-M-BSGP for WT and PG.
- [89] H. Alamri, I.M. Low, Mechanical properties and water absorption behaviour of recycled cellulose fibre reinforced epoxy composites, Polym. Test. 31 (2012) 620–628, https://doi.org/10.1016/j.polymertesting.2012.04.002.
- [90] F. Korkees, Moisture absorption behavior and diffusion characteristics of continuous carbon fiber reinforced epoxy composites: a review, Polym.-Plast. Technol. Eng. 62 (2023) 1789–1822, https://doi.org/10.1080/ 25740881.2023.2234461.
- [91] E.R. Pittman, L.E. Lamberson, Dynamic fracture behavior of hygrothermally degraded carbon epoxy composites, J. Compos. Mater. 56 (2022) 2239–2252.
- [92] P. Bazan, A. Rochman, K. Mroczka, K. Badura, M. Melnychuk, P. Nosal, et al., Composites based on PLA/PHBV blends with Nanocrystalline cellulose NCC: mechanical and thermal investigation, Materials (Basel) 17 (2024) 6036, https://doi.org/10.3390/ma17246036.

- [93] V. Abhilash, N. Rajender, K. Suresh, X-ray diffraction spectroscopy of polymer nanocomposites, Elsevier Inc., 2016, https://doi.org/10.1016/B978-0-323-40183-8.00014-8.
- [94] Z.D. Nasihin, M. Masruri, W. Warsito, A. Srihardyastutie, Preparation of Nanocellulose bioplastic with a gradation color of red and yellow, IOP Conf Ser Mater Sci Eng 833 (2020), https://doi.org/10.1088/1757-899X/833/1/012078.
- [95] S. Zainuddin, M.V. Hosur, Y. Zhou, A.T. Narteh, A. Kumar, S. Jeelani, Experimental and numerical investigations on flexural and thermal properties of nanoclay–epoxy nanocomposites, Mater. Sci. Eng. A 527 (2010) 7920–7926, https://doi.org/10.1016/j.msea.2010.08.078.
- [96] L. Zuo, W. Fan, Y. Zhang, L. Zhang, W. Gao, Y. Huang, et al., Graphene/montmorillonite hybrid synergistically reinforced polyimide composite aerogels with enhanced flame-retardant performance, Compos. Sci. Technol. 139 (2017) 57–63, https://doi.org/10.1016/j.compscitech.2016.12.008.
- [97] Y.-R. Son, S.-J. Park, Green preparation and characterization of graphene oxide/ carbon nanotubes-loaded carboxymethyl cellulose nanocomposites, Sci. Rep. 8 (2018) 17601, https://doi.org/10.1038/s41598-018-35984-2.
- [98] Z. Mohammed, A. Tcherbi-Narteh, S. Jeelani, Effect of graphene nanoplatelets and montmorillonite nanoclay on mechanical and thermal properties of polymer nanocomposites and carbon fiber reinforced composites, SN Appl. Sci. 2 (2020), https://doi.org/10.1007/s42452-020-03780-1.
- [99] M. Bulota, S. Sriubaite, A. Michud, K. Nieminen, M. Hughes, H. Sixta, et al., The fiber-matrix interface in Ioncell cellulose fiber composites and its implications for the mechanical performance, J. Appl. Polym. Sci. 138 (2021) 1–8, https://doi. org/10.1002/app.50306
- [100] M. Fernández-Álvarez, A. Moure, L.A. Delgado, J.J. Reinosa, J.F. Fernández, Raman spectroscopy study of the role of dispersion and interfaces in the improvement of the mechanical properties of epoxy-TiO2 composites, J. Mater. Res. Technol. 34 (2025) 1744–1758, https://doi.org/10.1016/j. jmrt.2024.12.181.
- [101] P. Dhar, A. Kumar, V. Katiyar, Magnetic cellulose nanocrystal based anisotropic polylactic acid nanocomposite films: influence on electrical, magnetic, thermal, and mechanical properties, ACS Appl. Mater. Interfaces 8 (2016) 18393–18409.
- [102] A.E. Lewandowska, S.J. Eichhorn, Quantification of the degree of mixing of cellulose nanocrystals in thermoplastics using Raman spectroscopy, J. Raman Spectrosc. 47 (2016) 1337–1342.
- [103] N. Djordjevic, A. Marinkovic, P. Zivkovic, D. Kovacevic, S. Dimitrijevic, V. Kokol, et al., Improving the packaging performance of low-density polyethylene with PCL/nanocellulose/copper(II)oxide barrier layer, Sci. Sinter. 50 (2018) 149–161, https://doi.org/10.2298/SOS1802149D.
- [104] G. Socrates, Infrared and raman characteristic group frequencies: tables and charts. John Wiley & Sons. 2004.
- [105] W. Österle, A. Giovannozzi, T. Gradt, I. Häusler, A. Rossi, B. Wetzel, et al., Exploring the potential of Raman spectroscopy for the identification of silicone oil residue and wear scar characterization for the assessment of tribofilm functionality. Tribol. Int. 90 (2015) 481–490.
- [106] S.G. Prolongo, A. Jimenez-Suarez, R. Moriche, A. Ureña, In situ processing of epoxy composites reinforced with graphene nanoplatelets, Compos. Sci. Technol. 86 (2013) 185–191, https://doi.org/10.1016/j.compscitech.2013.06.020.
- [107] M. Akter, H. Ozdemir, K. Bilisik, Epoxy/Graphene nanoplatelet (GNP) nanocomposites: an experimental study on tensile, compressive, and thermal properties, Polymers 16 (2024), https://doi.org/10.3390/polym16111483.
- [108] L. Völker-Pop, J.A.R. Agudo, C. Giehl, Combined rheology and spectroscopy methods to characterize the cure behavior of epoxy resins, AIP Conf. Proc. 2997 (2023) 030001, https://doi.org/10.1063/5.0159798.
- [109] U.P. Agarwal, Analysis of cellulose and lignocellulose materials by Raman spectroscopy: a review of the current status, Molecules 24 (2019), https://doi. org/10.3390/molecules/24091659
- [110] J. Naveen, M. Jawaid, E.S. Zainudin, M. Thariq Hameed Sultan, R. Yahaya, Improved mechanical and moisture-resistant properties of woven hybrid epoxy composites by graphene Nanoplatelets (GNP), Materials (Basel) (2019) 12, https://doi.org/10.3390/mal.2081.249.
- [111] S.C. Her, K.C. Zhang, Mode II fracture analysis of gnp/epoxy nanocomposite film on a substrate, Polymers 13 (2021), https://doi.org/10.3390/polym13162823.
- [112] J. Hou, W. Zhang, G. Cui, W. Chen, X. Wang, S. Wu, et al., The room temperature fracture behaviors of GNPs/TA15 composites by pre-sintering and hot extrusion, Materials (Basel) 16 (2023), https://doi.org/10.3390/ma16010318.
- [113] G.V. Vigneshwaran, B.P. Shanmugavel, R. Paskaramoorthy, S. Harish, Tensile, impact, and mode-I behaviour of glass fiber-reinforced polymer composite modified by graphene nanoplatelets, Arch Civ Mech Eng 20 (2020) 94, https://doi.org/10.1007/s43452-020-00099-x.
- [114] X. Jia, J. Zheng, S. Lin, W. Li, Q. Cai, G. Sui, et al., Highly moisture-resistant epoxy composites: an approach based on liquid nano-reinforcement containing well-dispersed activated montmorillonite, RSC Adv. 5 (2015) 44853–44864, https://doi.org/10.1039/C5RA06397C.
- [115] S.S. Nair, C. Dartiailh, D.B. Levin, N. Yan, Highly toughened and transparent biobased epoxy composites reinforced with cellulose nanofibrils, Polymers (Basel) 11 (2019), https://doi.org/10.3390/polym11040612.
- [116] C. Zhang, J. Cui, W. Sui, Y. Gong, H. Liu, Y. Ao, et al., High heat resistance, strength, and toughness of epoxy resin with cellulose nanofibers and structurally designed ionic liquid, Chem. Eng. J. 478 (2023) 147063.
- [117] A. Kesavulu, A. Mohanty, Investigation of the effect of graphene Nanoplatelet content on flexural behavior, surface roughness and water absorption of a graphene Nanoplatelets reinforced epoxy nanocomposites, J. Surf. Sci. Technol. 37 (2022) 35–42, https://doi.org/10.18311/jsst/2021/27393.